

# On Optimal Regularization Parameters via Bilevel Learning

Matthias J. Ehrhardt, Silvia Gazzola, and Sebastian J. Scott \*

Department of Mathematical Sciences, University of Bath, Claverton Down, BA2 7AY, UK

## Abstract

Variational regularization is commonly used to solve linear inverse problems, and involves augmenting a data fidelity by a regularizer. The regularizer is used to promote a priori information and is weighted by a regularization parameter. Selection of an appropriate regularization parameter is critical, with various choices leading to very different reconstructions. Classical strategies used to determine a suitable parameter value include the discrepancy principle and the L-curve criterion, and in recent years a supervised machine learning approach called bilevel learning has been employed. Bilevel learning is a powerful framework to determine optimal parameters and involves solving a nested optimization problem. While previous strategies enjoy various theoretical results, the well-posedness of bilevel learning in this setting is still an open question. In particular, a necessary property is positivity of the determined regularization parameter. In this work, we provide a new condition that better characterizes positivity of optimal regularization parameters than the existing theory. Numerical results verify and explore this new condition for both small and high-dimensional problems.

**Keywords:** Inverse problems; Machine learning; Variational regularization; Bilevel learning; Imaging; Regularization parameter

## 1 Introduction

Inverse problems are a class of mathematical problems where one is tasked to determine the input to a system given its output and some knowledge about the properties of said system. Such problems arise in many important science and engineering applications such as biomedical, astronomical, and seismic imaging [6, 9, 33, 44].

We consider the class of discrete linear inverse problems wherein we are interested in retrieving the exact input  $x^* \in \mathbb{R}^n$  given a matrix  $A \in \mathbb{R}^{m \times n}$ , and corrupted measurement  $y \in \mathbb{R}^m$  satisfying

$$y \approx Ax^*. \quad (1)$$

The challenge with inverse problems such as (1) is that almost all interesting applications are ill-posed in the sense of Hadamard [42], in that at least one of the following conditions regarding solutions is violated: existence; uniqueness; continuity with respect to the observed measurement

---

\*Corresponding author: ss2767@bath.ac.uk

$y$ . A classical approach to remedy the ill-posedness of (1) is via variational regularization [9, 21], wherein one solves a minimization problem such as

$$\min_{x \in \mathbb{R}^n} \left\{ \frac{1}{2} \|Ax - y\|^2 + \alpha \mathcal{R}(x) \right\}. \quad (2)$$

In (2) we consider the popular squared Euclidean distance data fidelity, which can be statistically motivated by considering the negative log likelihood of an additive Gaussian noise corruption of  $Ax^*$  [6]. The regularizer  $\mathcal{R} : \mathbb{R}^n \rightarrow \mathbb{R}$  is used to encourage a priori information of the ground truth  $x^*$  in reconstructions. Although smooth regularizers are used [9, 57], in recent years a popular non-smooth choice has been total variation (TV) [66] which encourages sharp edges in reconstructions. While TV has seen wide success, it is known to induce a staircasing artifact [64]. In an attempt to remedy this issue but capture the otherwise success of TV, an entire zoo of TV-like regularizers have been proposed [9, 12] which include those that build on higher-order derivatives such as second-order TV [60], incorporate non-local structure [38], infimal-convolution based approaches [18], and the total generalized variation [13]. Due to computational or theoretical reasons [35, 69], one may require a smooth approximation of such regularizers [47, 73]. We remark that there are a variety of other flavours of regularizers available, such as those that utilize convolutions [20] or a trained neural network [3, 55]. The balance between the data fidelity and regularizer in (2) is controlled by the regularization parameter  $\alpha \geq 0$ . It is crucial to determine a suitable value of  $\alpha$ , as a poor choice could lead to a noise dominated or oversmoothed reconstruction [43].

There are a variety of existing techniques to determine an appropriate regularization parameter value, such as the discrepancy principle [43], generalized cross validation [41], or the L-curve criterion [43]. Depending on the choice of regularizer and algorithm used to solve (2), efficient methods that yield appropriate parameter values can be achieved [35, 36, 53, 68]. In particular, there is no one-method-fits-all and rather each method works under different assumptions to varying degrees of success [5, 7, 11, 33, 40, 43].

An alternative is machine learning, wherein an optimal parameter is found by minimizing some appropriate loss function. This can be achieved via bilevel learning - a popular data-driven approach to determine hyperparameters [6, 24, 29, 52] which sits in the wider class of bilevel optimization [23, 70]. In this work, we put emphasis on the following class of bilevel learning problems:

$$\min_{\alpha \in \mathcal{P}} \left\{ \mathcal{J}(\alpha) := \frac{1}{2} \mathbb{E} \left[ \|x^\alpha(y) - x^*\|^2 \right] \right\} \quad (3a)$$

$$\text{subject to } x^\alpha(y) = \arg \min_{x \in \mathbb{R}^n} \left\{ \Phi_\alpha(x) := \frac{1}{2} \|Ax - y\|^2 + \alpha \mathcal{R}(x) \right\}, \quad (3b)$$

where  $\mathcal{P}$  is a parameter space e.g.  $\mathcal{P} = [0, \infty)$ . The expectation in (3a) is the total expectation and, unless specified otherwise in which case it will be denoted by a subscript, can be taken with respect to, say, some underlying distribution of the ground truth or noise (that is, however  $Ax^*$  is corrupted to yield  $y$  in (1)). We do not require any properties of these distributions other than the expectations being well defined. Minimization problem (3a) is referred to as the upper level problem, and (3b) the lower level problem. We remark that we demand neither existence nor uniqueness of solutions to the bilevel learning problem (3).

We consider minimizing the expected squared error in (3a) which is the most popular choice of loss function in bilevel learning [24], though other choices have been explored [29, 37]. By minimizing the expected squared error, the determined parameter should perform well on average.

While it is of theoretical importance to study the expected squared error upper level cost function, usually in practice we instead have a finite number of training data  $(x_k^*, y_k)$ ,  $k = 1, \dots, K$ . In this

scenario the upper level cost function will be the empirical risk,

$$\frac{1}{2K} \sum_{k=1}^K \|x^\alpha(y_k) - x_k^*\|^2,$$

and the bilevel learning problem would be solved to determine a regularization parameter that performs well on the training dataset. Then, given some unseen measurement data which is similar to the training data, we can expect a solution to (3) to be a reasonable choice of parameter and the variational problem (3b) can be solved.

Although the bilevel learning problem (3) is phrased to optimize over a scalar  $\alpha$ , the general framework extends to the multi-parameter setting, where  $\alpha$  would instead be interpreted as a vector. For example: to find the weights of a sum of different regularizers [28]; the sampling of the forward operator for MRI [69]; the weights in the field of experts model [20]; the choice of norm for the data fidelity and regularizer [22]; the parameters of an input-convex neural network acting as the regularizer [3, 55]. In this work we are interested in bilevel learning as a regularization parameter choice rule, so remain in the scalar setting.

Regarding how one solves a bilevel learning problem in general, if the parameter space  $\mathcal{P}$  is low-dimensional, one can efficiently determine optimal parameters via search methods [2, 16]. In the general multi-parameter case, however, a brute force search is not computationally feasible and other strategies must be employed. Many such approaches aim to calculate gradients of  $\mathcal{J}$  directly and use a gradient based approach to determine optimal parameters [24]. Although the minimizer  $x^\alpha(y)$  is in general non-differentiable with respect to the associated parameters, provided the lower level cost function is sufficiently smooth, so-called hypergradients of  $\mathcal{J}$  can be derived using the implicit function theorem [51, 67]. An issue with this approach is that exact solutions of the lower level problem are required but are often computed numerically in practice. While results are still promising in spite of this [69], methods that acknowledge this inexactness have also been developed and studied [31, 32, 75]. While some approaches try to bypass the smoothness assumption on  $\Phi_\alpha$  [58, 59], said methods only consider an approximation of the original bilevel problem and so must be handled with care.

A critical theoretical issue of (3) is the well-posedness of the learning and the characterization of solutions, which can be used to inform the design of numerical methods. In recent years, literature has been developed to address these issues [27, 28, 46, 52]. One example is [46], where the considered parameter space is  $\mathcal{P} = [\underline{\alpha}, \bar{\alpha}]$  for  $0 < \underline{\alpha} \leq \bar{\alpha} < \infty$  chosen a priori. In this setting it is possible to prove stability of the lower level problem and existence of solutions to the upper level problem under certain assumptions. However, in imposing solutions lie in a closed interval bounded away from 0 determined a priori, it is possible that for a given training dataset the determined parameter is suboptimal.

While a lot of existing theory and numerical methods for solving (3b) explicitly assume that the regularization parameter is non-zero [19, 22, 49], which would be in alignment with the setting of [46], in allowing  $\alpha$  to be zero, that is, to consider

$$\mathcal{P} = [0, \infty), \tag{4}$$

we will see that it is possible for 0 to be a solution to (3) for even the most simple problems. We commit to the choice of (4) from now on. Depending on the application, the choice of  $\alpha = 0$  can lead to degeneracy of (3b) such as non-uniqueness of minimizers. Furthermore, for an optimal parameter to be 0 may be an indication that the chosen regularizer is not well suited for the problem setting. Determining natural conditions which guarantee 0 is not a solution to (3) is therefore crucial to not only exclude these degenerate cases, but also to characterize suitability of regularizers for a given

application. Additionally, since the optimized parameter in (3) is the regularization parameter of a variational model, understanding when 0 is not a solution will help establish the validity of bilevel learning as a mathematically sound regularization parameter choice strategy, since positivity of the determined parameter is a necessary property [33]. Various works have contributed towards conditions that guarantee 0 is not a solution to (3) [27, 28, 52] and, while primarily considering the pointwise denoising setting, wherein  $A = I$  and there is no expectation in (3a), have considered regularizers such as generalized Tikhonov [52], TV-like and their Huber counterparts [28], and more recently a broad class of lower semicontinuous regularizers [27].

To ease notation, we will sometimes suppress the dependence of the reconstruction on the observed measurement, that is, denote  $x^\alpha(y)$  simply as  $x^\alpha$ , depending on what we want to emphasize.

## 1.1 Our contribution

In this work we provide a new sufficient condition to guarantee that 0 is not a solution to the bilevel learning problem (3) that is applicable to inverse problems with an injective forward operator, rather than just the denoising setting. In particular, the new condition ensures that a generalized directional derivative of  $\mathcal{J}$  at 0 is strictly negative for the class of lower level cost functions  $\Phi_\alpha$  for which the regularizer  $\mathcal{R}$  is real-valued, bounded below, convex, and continuously differentiable. We also provide an extension to the setting where the upper level cost function is the expected predicted risk and the forward operator is invertible. Full statements of the main results are provided in Section 2 and, after some preliminary results stated in Section 3, are proved in Section 4.

We show that, in the pointwise setting, data  $(x^*, y)$  that satisfy a condition commonly used to deduce positivity of optimal parameters [27, 28] immediately satisfy our new condition, which is empirically shown in Section 5 to be a better characterization of positivity. In allowing an expectation in the upper level problem, our setting is in contrast to existing work [27, 28, 52] where only a pointwise problem is considered. We show not only will our condition always be satisfied in a realistic denoising setting, but it can completely characterize positivity for certain applications.

## 2 Main results

The choice of regularizer is problem specific, as what constitutes as a suitable reconstruction varies between applications. In general,  $\mathcal{R}$  should attain a large evaluation for an  $x$  that exhibits undesirable properties. For the denoising application we have  $A = I$ , and are trying to improve upon the noisy measurement  $y$ . In particular,  $\mathcal{R}$  should deem  $y$  less desirable than the ground truth  $x^*$ . Thus, it is natural to assume that

$$\mathcal{R}(x^*) < \mathcal{R}(y). \quad (5)$$

Indeed, (5) has been considered in recent works [27, 28] to deduce positivity of solutions of the bilevel learning problem.

While we do not demand it here, typically the regularizer  $\mathcal{R}$  involves a norm and in particular is an even function. Consequently, for a fixed  $x^*$ , (5) is inherently circular around the origin and as such may fail to fully characterize the  $y$  for which 0 is not a solution to (3). While our condition will encompass applications with an injective forward operator, to give an intuition of how it compares to (5), in the denoising setting our condition will read as requiring the linearization of  $\mathcal{R}$  around  $y$  evaluated at  $x^*$  to be smaller than  $\mathcal{R}(y)$  to conclude that 0 is not a solution to (3). To represent this linearization, we will find it useful to work with Bregman distances, which are defined as follows.

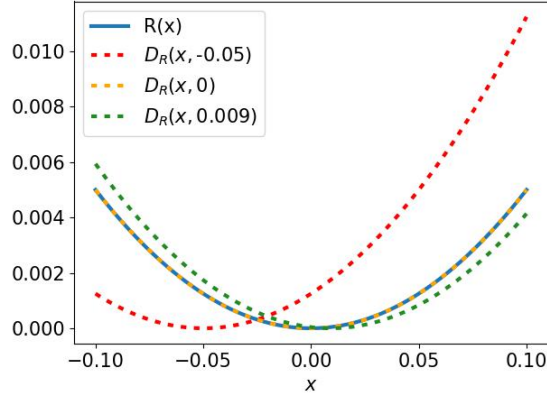


Figure 1: The case  $n = 1$ ,  $\mathcal{R}(x) = \frac{1}{2}\|x\|^2$ . Plot of regularizer evaluations and Bregman distances  $D_{\mathcal{R}}(\cdot, z)$  for different choices of  $z$ .

**Definition 1** (Bregman distance). For a differentiable convex function  $\psi : \mathbb{R}^n \rightarrow \mathbb{R}$  with gradient  $\nabla\psi$ , the Bregman distance is defined as

$$D_{\psi}(x, \tilde{x}) := \psi(x) - \psi(\tilde{x}) - \langle \nabla\psi(\tilde{x}), x - \tilde{x} \rangle.$$

Bregman distances can be considered a generalization of the squared Euclidean norm, and have nice properties such as convexity in the first argument and non-negativity [14]. We remark that while some definitions demand  $\psi$  be strictly convex [17], we do not require that here as convexity provides all the properties we need for the scope of this work. We now give a few examples of Bregman distances.

**Example 1.** Let  $\mathcal{R}(x) = \frac{1}{2}\|Lx\|^2$  where  $L \in \mathbb{R}^{p \times n}$ . One can show that the Bregman distance is given by

$$D_{\mathcal{R}}(x, z) = \frac{1}{2}\|L(x - z)\|^2.$$

For the case  $n = 1, L = I$ , a graph of  $\mathcal{R}$  and Bregman distances  $D_{\mathcal{R}}(\cdot, z)$  for different values of  $z$  is provided in Figure 1.

**Example 2.** Let  $n = 1$  and  $\mathcal{R}(x) = \text{hub}_{\gamma}(x)$  where

$$\text{hub}_{\gamma}(x) = \begin{cases} |x| - \frac{\gamma}{2} & \text{if } |x| \geq \gamma \\ \frac{1}{2\gamma}x^2 & \text{if } |x| < \gamma. \end{cases}$$

One can show that the Bregman distance is given by

$$D_{\mathcal{R}}(x, z) = \begin{cases} (\text{sign}(x) - \text{sign}(z))x & \text{if } |x| \geq \gamma, |z| \geq \gamma \\ x \left( \text{sign}(x) - \frac{1}{\gamma}z \right) + \frac{1}{2\gamma}z^2 - \frac{\gamma}{2} & \text{if } |x| \geq \gamma, |z| < \gamma \\ x \left( \frac{1}{2\gamma}x - \text{sign}(z) \right) + \frac{\gamma}{2} & \text{if } |x| < \gamma, |z| \geq \gamma \\ \frac{1}{2\gamma}(x - z)^2 & \text{if } |x| < \gamma, |z| < \gamma \end{cases}$$

For the case  $\gamma = 0.01$ , a graph of  $\mathcal{R}$  and Bregman distances  $D_{\mathcal{R}}(\cdot, z)$  for different values of  $z$  is provided in Figure 2.

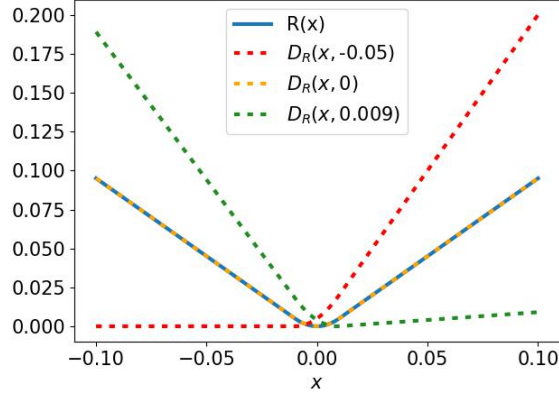


Figure 2: The case  $n = 1$ ,  $\mathcal{R}(x) = \text{hub}_\gamma(x)$ ,  $\gamma = 0.01$ . Plot of regularizer evaluations and Bregman distances  $D_{\mathcal{R}}(\cdot, z)$  for different choices of  $z$ .

From the definition of the Bregman distance, it is clear that, when viewed as a function of  $x$ , it represents the distance between  $\psi(x)$  and the linearization of  $\psi$  around  $\tilde{x}$  evaluated at  $x$ .

Rather than requiring  $A = I$  and (5), we merely require that  $A$  is injective and

$$\mathcal{R}(Bx^*) - D_{\mathcal{R}}(Bx^*, x^0) < \mathcal{R}(Bx^0) - D_{\mathcal{R}}(Bx^0, x^0), \quad (6)$$

where  $B := (A^T A)^{-1}$ , to deduce that 0 is not a solution to (3). A full statement of the result is provided in Theorem 1. Since  $A$  is injective,  $A^T A$  is invertible and  $x^0$  is the unique least-squares solution and so (6) is well-defined. An injective forward operator captures various relevant applications, such as certain convolutions and the Radon transform [54, 62]. If we are in the denoising setting and (5) is satisfied, we immediately get that (6) is also satisfied by the non-negativity of the Bregman distance. Figure 3a compares, for a fixed  $x^*$  and denoising application, how the region of possible  $x^0$  for which (5) and (6) are satisfied differ. Figure 3b provides a geometric interpretation of the new condition for a non-denoising application.

We now provide a motivating example illustrating that (6) can completely characterize whether 0 is a solution to (3).

**Example 3.** Consider the denoising setting with Tikhonov regularization,  $\mathcal{R} = \frac{1}{2}\|\cdot\|^2$ , and a single data sample. In this setting the lower level solution is given analytically as  $x^\alpha = y/(1 + \alpha)$ . Further, assume that  $\|y\| \neq 0$ ,  $\langle y, x^* \rangle > 0$ , and a solution to (3) exists. We claim that 0 is not a minimum if and only if (6) is satisfied.

Now, the solution to (3) will either be at the boundary or interior of  $\mathcal{P}$ . Evaluation of the upper level at the boundary yields

$$\mathcal{J}(0) = \frac{1}{2}\|y - x^*\|^2.$$

Optimal solutions  $\bar{\alpha}$  in the interior will satisfy  $0 = \mathcal{J}'(\bar{\alpha})$ , from which one can show that

$$\bar{\alpha} = \frac{\|y\|^2}{\langle y, x^* \rangle} - 1, \quad (7)$$

which is not strictly positive in general.

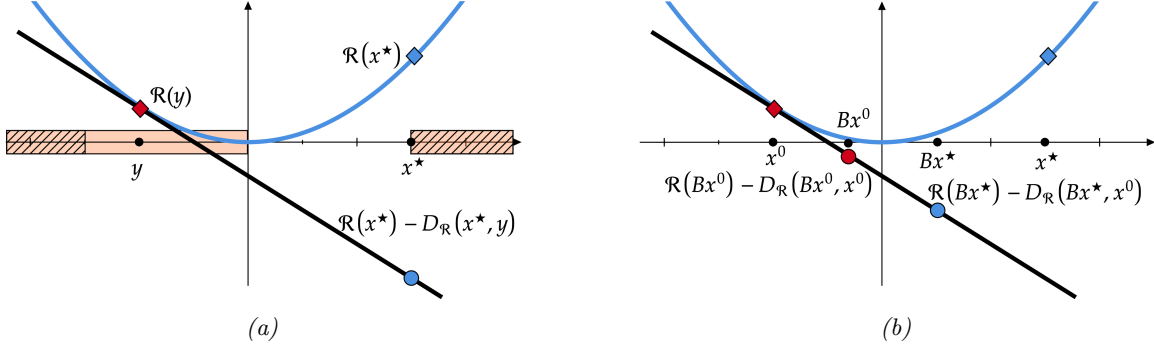


Figure 3: The case  $n = 1$ ,  $\mathcal{R}(x) = \frac{1}{2}\|x\|^2$ . (a) shows a plot of regularizer evaluations and illustration of the new condition in the case  $A = 1$ . While the old condition demands that the red diamond is higher than the blue diamond, the new condition only requires that the red diamond is higher than the blue circle. Regions of  $y$  for which the old and new conditions are satisfied are indicated by the striped and orange regions on the horizontal axis respectively. We see that the two conditions describe different regions and the striped region is a subset of the shaded region. (b) shows a plot of regularizer evaluations and illustration of the new condition in the case  $A = \sqrt{3}$ . The new condition only demands that the red circle is higher than the blue circle.

Suppose  $0$  is not a minimum of  $\mathcal{J}$ . Then  $\mathcal{J}(0) > \mathcal{J}(\bar{\alpha})$  with  $\bar{\alpha} > 0$ , and it follows from (7) that  $\bar{\alpha} > 0$  if and only if

$$\frac{1}{2}\|x^*\|^2 - \frac{1}{2}\|y - x^*\|^2 < \frac{1}{2}\|y\|^2,$$

that is, (6) is satisfied.

Suppose (6) is satisfied. By the above this is equivalent to  $\bar{\alpha} > 0$ . To deduce that  $0$  is not a minimum, it remains to show that  $\mathcal{J}(0) > \mathcal{J}(\bar{\alpha})$ . Indeed, the associated upper level cost of  $\bar{\alpha}$  is

$$\mathcal{J}(\bar{\alpha}) = \frac{1}{2}\|x^*\|^2 - \frac{1}{2} \frac{\langle y, x^* \rangle^2}{\|y\|^2}$$

and, since  $\bar{\alpha} > 0$ , it follows from (7) that

$$\begin{aligned} \frac{1}{2} \left( \frac{\langle y, x^* \rangle}{\|y\|} - \|y\| \right)^2 &> 0 \\ \iff \frac{1}{2}\|y - x^*\|^2 &> \frac{1}{2}\|x^*\|^2 - \frac{1}{2} \frac{\langle y, x^* \rangle^2}{\|y\|^2}, \end{aligned}$$

that is,  $\mathcal{J}(0) > \mathcal{J}(\bar{\alpha})$ .

To summarize, for a denoising problem with Tikhonov regularization, (6) is satisfied if and only if  $0$  is not a solution to (3).

The main result is the following.

**Theorem 1** (Positivity of the bilevel learning problem solution). *Let  $A$  be injective and let  $\mathcal{R}$  be convex, bounded below, and continuously differentiable. If*

$$\mathbb{E} [\mathcal{R}(Bx^*) - D_{\mathcal{R}}(Bx^*, x^0(y))] < \mathbb{E} [\mathcal{R}(Bx^0) - D_{\mathcal{R}}(Bx^0(y), x^0(y))] \quad (8)$$

and

$$\mathbb{E} [\mathcal{R}(Bx^\star) + D_{\mathcal{R}}(Bx^0(y), x^0(y))] < \infty,$$

then 0 is not a solution to (3).

The proof is provided in Section 4.

Since Theorem 1 can be considered a characterization of whether a regularizer is appropriate for a given application, ensuring (8) is satisfied could inform the design of new, or augmentation of existing regularizers for specific applications. Furthermore, we will later see that the difference between both sides of (8) will correspond to the steepness of a generalized directional derivative of  $\mathcal{J}$  at 0. Thus selecting  $\mathcal{R}$  such that not only is (8) satisfied, but

$$\mathbb{E} [\mathcal{R}(Bx^\star) - D_{\mathcal{R}}(Bx^\star, x^0)] \ll \mathbb{E} [\mathcal{R}(Bx^0) - D_{\mathcal{R}}(Bx^0, x^0)]$$

can be an indication that the choice of regularizer will yield noticeable improvement of reconstruction quality compared to the unregularized reconstruction.

We now state an immediate result of Theorem 1 for the pointwise setting, wherein  $(x^\star, y)$  is fixed and so there will be no expectation in the upper level (3a).

**Corollary 1.** *Let  $A$  be injective and let  $\mathcal{R}$  be convex, bounded below, and continuously differentiable. If  $x^\star \in \mathbb{R}^n$  and  $y \in \mathbb{R}^m$  are fixed and*

$$\mathcal{R}(Bx^\star) - D_{\mathcal{R}}(Bx^\star, x^0) < \mathcal{R}(Bx^0) - D_{\mathcal{R}}(Bx^0, x^0),$$

then 0 is not a solution to (3).

**Remark 1.** *For the special case of  $A = I$  and  $\mathcal{R}(x) = \frac{1}{2}\|Lx\|^2$  where  $L \in \mathbb{R}^{p \times n}$ , Corollary 1 is proven in [52, Proposition 3.1] where an equivalent condition,  $\langle L^T Ly, x^\star - y \rangle > 0$ , is assumed.*

Another corollary of Theorem 1 is that, for a realistic denoising problem, we are guaranteed that 0 is not a solution to (3).

**Corollary 2.** *Let  $A = I$  and let  $\mathcal{R}$  be convex, bounded below, and continuously differentiable. If  $x^\star$  is fixed and  $y = x^\star + \epsilon$  where  $\mathbb{E}_\epsilon[\epsilon] = 0$ , then we have the following.*

(i) Condition (8) is equivalent to

$$0 < \mathbb{E}_\epsilon [D_{\mathcal{R}}(y, x^\star) + D_{\mathcal{R}}(x^\star, y)]. \quad (9)$$

(ii) If  $\mathcal{R}$  is strictly convex, then 0 is not a solution to (3) almost surely.

The proof of Corollary 2 is provided in Section 4.

**Remark 2.** *The quantity in the expectation in (9) is called the symmetric Bregman distance. For details regarding properties and use of the symmetric Bregman distance in optimisation see, for example, [10, 15].*

Now the bilevel learning problem (3), and thus the result of Theorem 1, is specific to the expected squared error upper level cost, where access to clean samples  $x^\star$  is required. If direct access to  $x^\star$  is not be possible, one could instead consider a cost function based on the measurement space [30, 34, 45, 71, 74]. For this reason we will also consider an alternative upper level cost function, namely, the expected predictive risk,

$$\mathcal{J}(\alpha) = \mathbb{E} \left[ \frac{1}{2} \|Ax^\alpha - Ax^\star\|^2 \right],$$



where we will require that  $A$  is invertible. We leave the consideration of other cost functions as future work. In this setting, the associated bilevel learning problem is

$$\min_{\alpha \in \mathcal{P}} \mathbb{E} \left[ \frac{1}{2} \|Ax^\alpha - Ax^*\|^2 \right], \quad (10a)$$

$$\text{subject to } x^\alpha = \arg \min_{x \in \mathbb{R}^n} \left\{ \frac{1}{2} \|Ax - y\|^2 + \alpha \mathcal{R}(x) \right\}. \quad (10b)$$

Using Theorem 1 and the invertibility of  $A$ , positivity of solutions of the bilevel learning problem (10) can be established.

**Theorem 2.** *Let  $A$  be invertible and let  $\mathcal{R}$  be convex, bounded below, and continuously differentiable. If*

$$\mathbb{E} [\mathcal{R}(x^*) - D_{\mathcal{R}}(x^*, x^0(y))] < \mathbb{E} [\mathcal{R}(x^0(y))]$$

and

$$\mathbb{E} [\mathcal{R}(x^*)] < \infty,$$

then 0 is not a solution to (10).

The proof of Theorem 2 is provided in Section 4. We have an immediate corollary for the pointwise setting, wherein there is no expectation in the upper level (10a).

**Corollary 3.** *Let  $A$  be invertible and let  $\mathcal{R}$  be convex, bounded below, and continuously differentiable. If  $x^* \in \mathbb{R}^n$  and  $y \in \mathbb{R}^m$  are fixed and*

$$\mathcal{R}(x^*) - D_{\mathcal{R}}(x^*, x^0) < \mathcal{R}(x^0),$$

then 0 is not a solution to (10).

Before we prove the main results we first cover in Section 3 some fundamental results and properties of the lower level problem.

### 3 Preliminaries

We start by stating relevant definitions and properties of the lower level cost function. In particular, we require properties that are sufficient for existence and uniqueness of solutions to the lower level problem, as well as continuity of reconstructions with respect to the regularization parameter. The following definitions are taken from [8] and [19].

**Definition 2** (Minimizer). *We say that  $\hat{x}$  is a global minimizer of  $\psi : \mathbb{R}^n \rightarrow \mathbb{R}$  if  $\psi(\hat{x}) \leq \psi(x)$  for all  $x \in \mathbb{R}^n$ .*

**Definition 3** (Bounded below). *A function  $\psi : \mathbb{R}^n \rightarrow \mathbb{R}$  is bounded below if there exists  $C \in \mathbb{R}$  such that*

$$\psi(x) \geq C \quad \text{for all } x \in \mathbb{R}^n.$$

**Definition 4** (Coercive). *A function  $\psi : \mathbb{R}^n \rightarrow \mathbb{R}$  is coercive if*

$$\psi(x) \rightarrow \infty \quad \text{as } \|x\| \rightarrow \infty.$$

**Definition 5** (Convex function). A function  $\psi : \mathbb{R}^n \rightarrow \mathbb{R}$  is said to be convex if for all  $x, z \in \mathbb{R}^n$ ,

$$D_\psi(x, z) \geq 0. \quad (11)$$

Moreover,  $\psi$  is said to be strictly convex if for  $x \neq z$ , inequality (11) is strict.

**Remark 3.** The classical definition of (strict) convexity [61] is different to the one we use, however it can be easily recovered by the definition of the Bregman distance (e.g. see [61, Proposition 3.10]).

We can now state a classical result regarding existence and uniqueness of minimizers.

**Lemma 1.** Let  $\psi : \mathbb{R}^n \rightarrow \mathbb{R}$  be bounded below, coercive, and strictly convex. Then  $\psi$  has a unique global minimizer.

*Proof.* Since  $\psi$  is convex and real-valued it is continuous (see [65, Corollary 10.1.1]). Existence follows from the direct method in the calculus of variations [25]. Uniqueness follows by strict convexity.  $\square$

In particular, by the assumptions on  $A$  and  $\mathcal{R}$ , the lower level problem (3b) admits a unique minimizer, justifying our choice of notation.

**Proposition 1** (Properties of the lower level cost function). Fix  $\alpha \geq 0$ . Let  $A$  be injective and let  $\mathcal{R}$  be convex, bounded below, and continuously differentiable. Then the lower level cost function  $\Phi_\alpha$  is bounded below, coercive, continuous, and strictly convex. Moreover, it admits a unique global minimizer.

*Proof.* The properties of  $\Phi_\alpha$  follow from standard results in convex analysis. Existence and uniqueness of a minimizer follows from Lemma 1.  $\square$

We require continuity of the reconstruction map  $\alpha \mapsto x^\alpha$  at  $\alpha = 0$ . Although this is a well studied result [26, 28], we include a full proof for completeness.

**Lemma 2** (Convergence of reconstructions at the boundary). Let  $A$  be injective and let  $\mathcal{R}$  be convex, bounded below, and continuously differentiable. If  $\{\alpha_k\} \subset (0, \infty)$  satisfies  $\lim_{k \rightarrow \infty} \alpha_k = 0$  then  $\lim_{k \rightarrow \infty} x^{\alpha_k} = x^0$ .

*Proof.* By the choice of datafit  $\mathcal{F}(x) = \frac{1}{2} \|Ax - y\|^2$  and injectivity of  $A$ ,  $x^0$  is the unique minimizer of  $\mathcal{F}$ . By the minimality of  $x^0$

$$\mathcal{F}(x^0) \leq \mathcal{F}(x^{\alpha_k})$$

and since  $\mathcal{R}$  is bounded below by some  $C \in \mathbb{R}$

$$\begin{aligned} \mathcal{F}(x^{\alpha_k}) &\leq \mathcal{F}(x^{\alpha_k}) + \alpha_k(\mathcal{R}(x^{\alpha_k}) - C) \\ &= \Phi_{\alpha_k}(x^{\alpha_k}) - \alpha_k C. \end{aligned}$$

By the minimality of  $x^{\alpha_k}$ ,

$$\begin{aligned} \Phi_{\alpha_k}(x^{\alpha_k}) - \alpha_k C &\leq \Phi_{\alpha_k}(x^0) - \alpha_k C \\ &= \mathcal{F}(x^0) + \alpha_k(\mathcal{R}(x^0) - C). \end{aligned}$$

In particular, we have

$$\mathcal{F}(x^0) \leq \mathcal{F}(x^{\alpha_k}) \leq \mathcal{F}(x^0) + \alpha_k(\mathcal{R}(x^0) - C).$$

Since  $\mathcal{R}(x^0)$  and  $C$  are fixed and  $\alpha_k \rightarrow 0$ , we see that  $\lim_{k \rightarrow \infty} \mathcal{F}(x^{\alpha_k}) = \mathcal{F}(x^0)$ . By continuity of the datafit and both minimality and uniqueness of  $x^0$ , it follows that  $\lim_{k \rightarrow \infty} x^{\alpha_k} = x^0$  and we are done.  $\square$

## 4 Proof of the main results

We aim to characterize when  $\alpha = 0$  is not a local minimum of the upper level cost function  $\mathcal{J}$  by studying local behaviour of  $\mathcal{J}$  around 0. There are two main challenges towards this: firstly, the reconstruction map  $\alpha \mapsto x^\alpha$  is in general non-differentiable [48] and consequently, without stronger assumptions on the choice of regularizer  $\mathcal{R}$  [67, 69], the upper level cost function  $\mathcal{J}$  is non-differentiable; secondly, the value we are interested in is on the domain boundary of  $\mathcal{J}$ . To this end, we work with a generalization of the derivative known as Dini derivatives [4, 39, 50]. More precisely, we consider the upper right Dini derivative.

**Definition 6** (Upper right Dini derivative). *Let  $\mathcal{J}$  be any real-valued function defined on  $[0, \infty)$  and let  $\tilde{\alpha} \geq 0$ . We define the upper right Dini derivative of  $\mathcal{J}$  evaluated at  $\tilde{\alpha}$  as*

$$\mathcal{J}'_+(\tilde{\alpha}) := \limsup_{\alpha \rightarrow \tilde{\alpha}_+} \frac{\mathcal{J}(\alpha) - \mathcal{J}(\tilde{\alpha})}{\alpha - \tilde{\alpha}},$$

where  $\alpha \rightarrow \tilde{\alpha}_+$  denotes the right-hand limit.

We remark that we allow infinite limits in the above definition and so the upper right Dini derivative is always well defined. Dini derivatives follow some standard calculus rules and generalizations of the mean value theorem and Rolle's theorem can be stated [4, 39, 50].

For clarity, we state precisely what we mean for a point to be a local minimum.

**Definition 7** (Local minimum). *Let  $\mathcal{J} : [0, \infty) \rightarrow \mathbb{R}$  be any function. We say that  $\alpha^* \geq 0$  is a local minimum of  $\mathcal{J}$  if there exists  $\delta > 0$  such that*

$$\mathcal{J}(\alpha^*) \leq \mathcal{J}(\alpha) \quad \text{for all } \alpha \in [\alpha^* - \delta, \alpha^* + \delta] \cap [0, \infty).$$

We now use Dini derivatives to determine behaviour of  $\mathcal{J}$  at the domain boundary.

**Lemma 3.** *Let  $\mathcal{J} : [0, \infty) \rightarrow \mathbb{R}$  be any function. If the upper right Dini derivative at 0 satisfies  $\mathcal{J}'_+(0) < 0$  then 0 is not a local minimum of  $\mathcal{J}$ .*

*Proof.* Assume  $\mathcal{J}'_+(0) < 0$ . We then have existence of  $\delta > 0$  such that

$$\frac{\mathcal{J}(\alpha) - \mathcal{J}(0)}{\alpha} < 0$$

for all  $\alpha \in (0, \delta)$ . It immediately follows that  $\mathcal{J}(\alpha) < \mathcal{J}(0)$  in  $(0, \delta)$  and so  $\mathcal{J}$  is locally strictly decreasing at the domain boundary. In particular, 0 is not a local minimum of  $\mathcal{J}$ .  $\square$

**Remark 4.** *The condition in Lemma 3 is sufficient but not necessary for 0 to not be a minimizer of  $\mathcal{J}$ . Indeed, we will see in Section 5 that the upper level cost function (3a) is non-convex and in particular 0 may actually be a local minimum, and yet global minima of (3a) are achieved at strictly positive parameter values.*

We now prove the result of Theorem 1 in Section 4.1 and, using the result of Theorem 1, prove Theorem 2 in Section 4.2.

#### 4.1 Proof of Theorem 1

Motivated by Lemma 3, we aim to rewrite  $\mathcal{J}(\alpha) - \mathcal{J}(0)$  in a more desirable form, such that the division by  $\alpha$  in the Dini derivative will be easier to handle. While the bilevel learning problem (3) involves an expectation, we will find it useful to work with the quantity that we are taking the expectation of and to this end define

$$\tilde{\mathcal{J}}(\alpha) := \frac{1}{2} \|x^\alpha - x^\star\|^2,$$

and so clearly  $\mathcal{J}(\alpha) = \mathbb{E}[\tilde{\mathcal{J}}(\alpha)]$ . We focus on calculating  $\tilde{\mathcal{J}}'_+(0)$  and build on those results to prove Theorem 1. Now, we would ideally like to rewrite  $\tilde{\mathcal{J}}(\alpha) - \tilde{\mathcal{J}}(0)$  of the form  $\alpha h(\alpha)$  for some  $h$  such that  $\tilde{\mathcal{J}}'_+(0) = \limsup_{\alpha \rightarrow 0+} h(\alpha) < 0$ . While such a form will not be fully achieved, we will determine a form such that the terms that do not have a factor of  $\alpha$  will still vanish in the relevant limit. More precisely, we want to make a connection between the upper right Dini derivative and regularizer evaluations, and will achieve this using Bregman distances and optimality conditions of  $x^\alpha$ . In particular, we will use the following property of the gradient.

**Proposition 2.** *Let  $\mathcal{R}$  be convex, bounded below, and continuously differentiable and let  $x^0$  be any least squares solution. Then*

$$\alpha \nabla \mathcal{R}(x^\alpha) = A^T A x^0 - A^T A x^\alpha. \quad (12)$$

*Proof.* By the choice of the data fidelity and differentiability of  $\mathcal{R}$ , we have that

$$0 = \nabla \Phi_\alpha(x^\alpha) = A^T A x^\alpha - A^T y + \alpha \nabla \mathcal{R}(x^\alpha). \quad (13)$$

Since  $x^0$  is a least squares solution, it satisfies the normal equations

$$A^T A x^0 - A^T y = 0. \quad (14)$$

Combining (13) and (14) yields (12).  $\square$

We now state the form of  $\tilde{\mathcal{J}}(\alpha) - \tilde{\mathcal{J}}(0)$  that will be utilized.

**Proposition 3.** *Let  $A$  be injective and let  $\mathcal{R}$  be convex, bounded below, and continuously differentiable. Then*

$$\tilde{\mathcal{J}}(\alpha) - \tilde{\mathcal{J}}(0) = \alpha \langle \nabla \mathcal{R}(x^\alpha), Bx^\star - Bx^\alpha \rangle - \frac{1}{2} \|x^0 - x^\alpha\|^2.$$

*Proof.* By the definition of  $\tilde{\mathcal{J}}$  we have

$$\tilde{\mathcal{J}}(\alpha) = \frac{1}{2} \|x^\alpha - x^\star\|^2 = \frac{1}{2} \|x^\alpha\|^2 - \langle x^\alpha, x^\star \rangle + \frac{1}{2} \|x^\star\|^2$$

and in particular

$$\begin{aligned} \tilde{\mathcal{J}}(\alpha) - \tilde{\mathcal{J}}(0) &= \frac{1}{2} \|x^\alpha - x^\star\|^2 - \frac{1}{2} \|x^0 - x^\star\|^2 \\ &= \frac{1}{2} \|x^\alpha\|^2 - \frac{1}{2} \|x^0\|^2 + \langle x^0 - x^\alpha, x^\star \rangle \\ &= \frac{1}{2} \|x^\alpha\|^2 - \frac{1}{2} \|x^0\|^2 + \langle x^0 - x^\alpha, x^\star - x^\alpha \rangle + \langle x^0, x^\alpha \rangle - \langle x^\alpha, x^\alpha \rangle \\ &= \langle x^0 - x^\alpha, x^\star - x^\alpha \rangle - \frac{1}{2} \|x^0\|^2 + \langle x^0, x^\alpha \rangle - \frac{1}{2} \|x^\alpha\|^2 \\ &= \langle x^0 - x^\alpha, x^\star - x^\alpha \rangle - \frac{1}{2} \|x^0 - x^\alpha\|^2. \end{aligned}$$

It remains to show that

$$\langle x^0 - x^\alpha, x^\star - x^\alpha \rangle = \alpha \langle \nabla \mathcal{R}(x^\alpha), Bx^\star - Bx^\alpha \rangle.$$

Recall that, by Proposition 2,  $\alpha \nabla \mathcal{R}(x^\alpha)$  involves  $A^T A$  which we can freely introduce since it is invertible by the injectivity of  $A$ . Indeed,

$$\langle x^0 - x^\alpha, x^\star - x^\alpha \rangle = \langle B(A^T A)(x^0 - x^\alpha), x^\star - x^\alpha \rangle.$$

By the symmetry of  $B = (A^T A)^{-1}$

$$\langle B(A^T A)(x^0 - x^\alpha), x^\star - x^\alpha \rangle = \langle A^T A(x^0 - x^\alpha), B(x^\star - x^\alpha) \rangle.$$

Finally, by Proposition 2

$$\langle A^T A(x^0 - x^\alpha), B(x^\star - x^\alpha) \rangle = \alpha \langle \nabla \mathcal{R}(x^\alpha), Bx^\star - Bx^\alpha \rangle$$

and we are done.  $\square$

In calculating the upper right Dini derivative of  $\tilde{\mathcal{J}}$  at 0, we see from Proposition 3 that the quantity

$$\liminf_{\alpha \rightarrow 0_+} \frac{1}{\alpha} \|x^0 - x^\alpha\|^2 \quad (15)$$

will be encountered. As hinted earlier, we will show that (15) vanishes. Before we do this, we require two intermediate results.

**Proposition 4.** *Let  $\mathcal{R}$  be convex, bounded below, and continuously differentiable and let  $x^0$  be any least squares solution. Then*

$$\alpha(\mathcal{R}(x^0) - \mathcal{R}(x^\alpha)) \geq \|A(x^0 - x^\alpha)\|^2.$$

*Proof.* By the convexity of  $\mathcal{R}$  and definition of  $D_{\mathcal{R}}$ ,

$$\alpha(\mathcal{R}(x) - \mathcal{R}(x^\alpha)) \geq \langle \alpha \nabla \mathcal{R}(x^\alpha), x - x^\alpha \rangle.$$

By Proposition 2,

$$\langle \alpha \nabla \mathcal{R}(x^\alpha), x - x^\alpha \rangle = \langle A^T A x^0 - A^T A x^\alpha, x - x^\alpha \rangle$$

so in taking  $x = x^0$  we see that

$$\alpha(\mathcal{R}(x^0) - \mathcal{R}(x^\alpha)) \geq \|A(x^0 - x^\alpha)\|^2$$

and we are done.  $\square$

**Lemma 4.** *Let  $f, g : [0, \infty) \rightarrow \mathbb{R}$  be functions such that  $f(\alpha) \leq g(\alpha)$  for all  $\alpha \geq 0$ . Then*

$$\limsup_{\alpha \rightarrow 0_+} \frac{f(\alpha)}{\alpha} \leq \limsup_{\alpha \rightarrow 0_+} \frac{g(\alpha)}{\alpha}.$$

The proof of Lemma 4 is omitted as it follows from the definition of the lim sup and standard arguments in analysis. We now show that (15) vanishes.

**Proposition 5.** *Let  $A$  be injective and let  $\mathcal{R}$  be convex, bounded below, and continuously differentiable. Then*

$$\lim_{\alpha \rightarrow 0_+} \frac{1}{\alpha} \|x^0 - x^\alpha\|^2 = 0.$$

*Proof.* By the non-negativity of  $\|x^0 - x^\alpha\|^2/\alpha$ , we immediately have

$$0 \leq \limsup_{\alpha \rightarrow 0_+} \frac{1}{\alpha} \|x^0 - x^\alpha\|^2$$

and so the result will follow if we can show that

$$\limsup_{\alpha \rightarrow 0_+} \frac{1}{\alpha} \|x^0 - x^\alpha\|^2 \leq 0. \quad (16)$$

Since  $A$  is injective, we have that

$$\|x^0 - x^\alpha\|^2 \leq \frac{1}{\sigma_{\min}^2} \|A(x^0 - x^\alpha)\|^2,$$

where  $\sigma_{\min} > 0$  is the smallest singular value of  $A$ . Thus it suffices to show that

$$\limsup_{\alpha \rightarrow 0_+} \frac{1}{\alpha} \|A(x^0 - x^\alpha)\|^2 \leq 0, \quad (17)$$

as then the result will follow by Lemma 4. By Proposition 4 and Lemma 4

$$\limsup_{\alpha \rightarrow 0_+} \frac{1}{\alpha} \|A(x^0 - x^\alpha)\|^2 \leq \limsup_{\alpha \rightarrow 0_+} (\mathcal{R}(x^0) - \mathcal{R}(x^\alpha)) = 0,$$

where the equality follows by the continuity of  $\mathcal{R}$  and Lemma 2. In particular we have shown (17) and by Lemma 4 we have (16) and we are done.  $\square$

We are now ready to prove a crucial result for the proof of Theorem 1. In particular, we show that the upper right Dini derivative of  $\tilde{\mathcal{J}}$  at 0 can be given exactly in terms of Bregman distances and evaluations of the regularizer.

**Lemma 5.** *Let  $A$  be injective and let  $\mathcal{R}$  be convex, bounded below, and continuously differentiable. Then*

$$\tilde{\mathcal{J}}'_+(0) = \mathcal{R}(Bx^\star) - D_{\mathcal{R}}(Bx^\star, x^0) - \mathcal{R}(Bx^0) + D_{\mathcal{R}}(Bx^0, x^0).$$

*Proof.* By Proposition 3,

$$\begin{aligned} \tilde{\mathcal{J}}'_+(0) &= \limsup_{\alpha \rightarrow 0_+} \frac{\tilde{\mathcal{J}}(\alpha) - \tilde{\mathcal{J}}(0)}{\alpha} \\ &= \limsup_{\alpha \rightarrow 0_+} \left( \langle \nabla \mathcal{R}(x^\alpha), Bx^\star - Bx^\alpha \rangle - \frac{1}{2\alpha} \|x^0 - x^\alpha\|^2 \right). \end{aligned} \quad (18)$$

The last term in (18) will vanish in the limit by Proposition 5. By the continuity of  $\nabla \mathcal{R}$  and Lemma 2,

$$\begin{aligned} \tilde{\mathcal{J}}'_+(0) &= \langle \nabla \mathcal{R}(x^0), Bx^\star - Bx^0 \rangle \\ &= \langle \nabla \mathcal{R}(x^0), Bx^\star - x^0 + x^0 - Bx^0 \rangle \\ &= \mathcal{R}(Bx^\star) - \mathcal{R}(Bx^\star) + \langle \nabla \mathcal{R}(x^0), Bx^\star - x^0 \rangle - \mathcal{R}(Bx^0) + \mathcal{R}(Bx^0) \\ &\quad - \langle \nabla \mathcal{R}(x^0), Bx^0 - x^0 \rangle \\ &= \mathcal{R}(Bx^\star) - D_{\mathcal{R}}(Bx^\star, x^0) - \mathcal{R}(Bx^0) + D_{\mathcal{R}}(Bx^0, x^0) \end{aligned}$$

and we are done.  $\square$

Before we prove Theorem 1, we require an analogous result of Lemma 5 for the expected case where, unlike the pointwise setting, we will only be able to find an upper bound of  $\mathcal{J}'_+(0)$ .

**Lemma 6.** *Let  $A$  be injective and let  $\mathcal{R}$  be convex, bounded below, and continuously differentiable. If*

$$\mathbb{E} [\mathcal{R}(Bx^\star) + D_{\mathcal{R}}(Bx^0(y), x^0(y))] < \infty \quad (19)$$

then  $\mathcal{J}'_+(0) \leq \mathbb{E} [\tilde{\mathcal{J}}'_+(0)]$ .

*Proof.* The main challenge is to justify swapping the expectation and lim sup in

$$\mathcal{J}'_+(0) = \limsup_{\alpha \rightarrow 0_+} \mathbb{E} \left[ \frac{\tilde{\mathcal{J}}(\alpha) - \tilde{\mathcal{J}}(0)}{\alpha} \right].$$

This can be justified (up to inequality) by the Reverse Fatou Lemma (e.g. see [63, Corollary 5.3.2]). We now show that the conditions of the Reverse Fatou Lemma are satisfied, which in this setting requires showing that  $(\tilde{\mathcal{J}}(\alpha) - \tilde{\mathcal{J}}(0))/\alpha \leq Z$  for some random variable  $Z$  independent of  $\alpha$  satisfying  $\mathbb{E}[|Z|] < \infty$ .

By Proposition 3 and the definition of the Bregman distance (see also the proof of Lemma 5), we have

$$\begin{aligned} \tilde{\mathcal{J}}(\alpha) - \tilde{\mathcal{J}}(0) &\leq \alpha \langle \nabla \mathcal{R}(x^\alpha), Bx^\star - Bx^\alpha \rangle \\ &= \alpha (\mathcal{R}(Bx^\star) - D_{\mathcal{R}}(Bx^\star, x^\alpha) - \mathcal{R}(Bx^\alpha) + D_{\mathcal{R}}(Bx^\alpha, x^\alpha)). \end{aligned}$$

Since  $\mathcal{R}$  is bounded below by some  $C \in \mathbb{R}$  and  $D_{\mathcal{R}}$  is non-negative it follows that

$$\frac{\tilde{\mathcal{J}}(\alpha) - \tilde{\mathcal{J}}(0)}{\alpha} \leq h(\alpha) := \mathcal{R}(Bx^\star) - C + D_{\mathcal{R}}(Bx^\alpha, x^\alpha).$$

Notice that by the assumptions on  $\mathcal{R}$ , for any  $\alpha \geq 0$  we have that  $h(\alpha) \geq 0$ . By Lemma 2 and the continuity of  $\mathcal{R}$  and  $\nabla \mathcal{R}$ ,

$$\lim_{\alpha \rightarrow 0_+} h(\alpha) = h(0)$$

and so there exists  $\delta > 0$  such that for all  $\alpha \in [0, \delta]$ ,

$$h(\alpha) \leq h(0) + 1 =: Z.$$

We claim that this choice of  $Z$  is appropriate for the Reverse Fatou Lemma. Indeed, since we are only interested in behaviour of  $\mathcal{J}$  (and consequently  $\tilde{\mathcal{J}}$ ) at 0 we can, without loss of generality, restrict  $\mathcal{J}$  to  $[0, \delta]$ . Notice that  $Z > 0$  and so  $\mathbb{E}[|Z|] = \mathbb{E}[Z] < \infty$  by assumption (19). It then follows from the Reverse Fatou Lemma that

$$\mathcal{J}'_+(0) \leq \mathbb{E} \left[ \limsup_{\alpha \rightarrow 0_+} \frac{\tilde{\mathcal{J}}(\alpha) - \tilde{\mathcal{J}}(0)}{\alpha} \right] = \mathbb{E} [\tilde{\mathcal{J}}'_+(0)]$$

and we are done.  $\square$

We can now prove the main result, which for convenience we restate.

**Theorem 1** (Positivity of the bilevel learning problem solution). *Let  $A$  be injective and let  $\mathcal{R}$  be convex, bounded below, and continuously differentiable. If*

$$\mathbb{E} [\mathcal{R}(Bx^*) - D_{\mathcal{R}}(Bx^*, x^0(y))] < \mathbb{E} [\mathcal{R}(Bx^0) - D_{\mathcal{R}}(Bx^0(y), x^0(y))] \quad (20)$$

and

$$\mathbb{E} [\mathcal{R}(Bx^*) + D_{\mathcal{R}}(Bx^0(y), x^0(y))] < \infty, \quad (21)$$

then 0 is not a solution to (3).

*Proof.* By the assumptions we have from Lemma 6 that  $\mathcal{J}'_+(0) \leq \mathbb{E}[\tilde{\mathcal{J}}'_+(0)]$ . By assumption (20) and Lemma 5, we see that  $\mathcal{J}'_+(0) < 0$ . It follows from Lemma 3 that 0 is not a local minimizer of  $\mathcal{J}$  and in particular cannot be a global minimizer.  $\square$

We now show that, in the denoising setting where the measurement has been corrupted by additive noise of mean zero, if the regularizer is strictly convex then we are guaranteed that 0 is not a solution to (3).

**Corollary 2.** *Let  $A = I$  and let  $\mathcal{R}$  be convex, bounded below, and continuously differentiable. If  $x^*$  is fixed and  $y = x^* + \epsilon$  where  $\mathbb{E}_\epsilon[\epsilon] = 0$ , then we have the following.*

(i) *Condition (20) is equivalent to*

$$0 < \mathbb{E}_\epsilon [D_{\mathcal{R}}(y, x^*) + D_{\mathcal{R}}(x^*, y)]. \quad (22)$$

(ii) *If  $\mathcal{R}$  is strictly convex, then 0 is not a solution to (3) almost surely.*

*Proof.* By the definition of the Bregman distance, (20) is also given by

$$\begin{aligned} 0 &< \mathbb{E}_\epsilon [\langle \nabla \mathcal{R}(y), y - x^* \rangle] \\ &= \mathbb{E}_\epsilon [\langle \nabla \mathcal{R}(y) - \nabla \mathcal{R}(x^*) + \nabla \mathcal{R}(x^*), y - x^* \rangle] \\ &= \mathbb{E}_\epsilon [\langle \nabla \mathcal{R}(y) - \nabla \mathcal{R}(x^*), y - x^* \rangle + \langle \nabla \mathcal{R}(x^*), y - x^* \rangle]. \end{aligned} \quad (23)$$

In the denoising setting we have that  $y - x^* = \epsilon$ . Since  $x^*$  is fixed and  $\mathbb{E}_\epsilon[\epsilon] = 0$ , it follows from (23) that

$$\begin{aligned} 0 &< \mathbb{E}_\epsilon [\langle \nabla \mathcal{R}(y) - \nabla \mathcal{R}(x^*), y - x^* \rangle] + \langle \nabla \mathcal{R}(x^*), \mathbb{E}_\epsilon[\epsilon] \rangle \\ &= \mathbb{E}_\epsilon [\langle \nabla \mathcal{R}(y) - \nabla \mathcal{R}(x^*), y - x^* \rangle]. \end{aligned}$$

By definition of the Bregman distance, we have

$$\mathbb{E}_\epsilon [\langle \nabla \mathcal{R}(y) - \nabla \mathcal{R}(x^*), y - x^* \rangle] = \mathbb{E} [D_{\mathcal{R}}(y, x^*) + D_{\mathcal{R}}(x^*, y)]$$

and we have shown (22). Since  $\epsilon$  is a continuous random variable we have that  $x^* \neq y$  almost surely. From the definition of strict convexity it immediately follows that  $D_{\mathcal{R}}(y, x^*) > 0$  and so (22) is satisfied almost surely. Since  $A = I$  and  $x^*$  is fixed, the other condition of Theorem 1 is trivially satisfied and so 0 is not a minimum of (3) by Theorem 1.  $\square$

We now provide a sufficient condition for assumption (21) to be satisfied.



**Proposition 6.** *Let  $A$  be injective and let  $\mathcal{R}$  be convex, bounded below, continuously differentiable, and  $\beta$ -smooth, in that, for any  $x, z \in \mathbb{R}^n$*

$$\|\nabla \mathcal{R}(x) - \nabla \mathcal{R}(z)\| \leq \beta \|x - z\|.$$

If

$$\mathbb{E} [\mathcal{R}(Bx^*)] < \infty \quad \text{and} \quad \mathbb{E} [\|x^0(y)\|^2] < \infty, \quad (24)$$

then (21) is satisfied.

*Proof.* By the definition of the Bregman distance it follows from [8, Theorem 5.8] that  $\beta$ -smoothness is equivalent to

$$D_{\mathcal{R}}(x, z) \leq \frac{\beta}{2} \|x - z\|.$$

It follows that

$$\begin{aligned} \mathbb{E} [\mathcal{R}(Bx^*) + D_{\mathcal{R}}(Bx^0, x^0)] &\leq \mathbb{E} [\mathcal{R}(Bx^*)] + \frac{\beta}{2} \mathbb{E} [\|(B - I)x^0\|^2] \\ &\leq \mathbb{E} [\mathcal{R}(Bx^*)] + \frac{\beta \sigma_{\max}^2}{2} \mathbb{E} [\|x^0\|^2] \end{aligned}$$

where  $\sigma_{\max} \geq 0$  is the largest singular value of  $B - I$ . Thus (24) is sufficient for (21) to be satisfied.  $\square$

## 4.2 Proof of Theorem 2

We now prove an analogous result of Theorem 1 for the predictive risk upper level cost function and an invertible forward operator  $A$ , wherein the associated bilevel learning problem is

$$\min_{\alpha \in \mathcal{P}} \mathbb{E} \left[ \frac{1}{2} \|Ax^\alpha - Ax^*\|^2 \right], \quad (25a)$$

$$\text{subject to } x^\alpha = \arg \min_{x \in \mathbb{R}^n} \left\{ \frac{1}{2} \|Ax - y\|^2 + \alpha \mathcal{R}(x) \right\}. \quad (25b)$$

Using Theorem 1 and the invertibility of  $A$ , positivity of solutions of the bilevel learning problem (25) can be established.

**Theorem 2.** *Let  $A$  be invertible and let  $\mathcal{R}$  be convex, bounded below, and continuously differentiable. If*

$$\mathbb{E} [\mathcal{R}(x^*) - D_{\mathcal{R}}(x^*, x^0(y))] < \mathbb{E} [\mathcal{R}(x^0(y))] \quad (26)$$

and

$$\mathbb{E} [\mathcal{R}(x^*)] < \infty, \quad (27)$$

then 0 is not a solution to (25).

*Proof.* Using the invertibility of  $A$ , we intend to rephrase the bilevel learning problem (25) as a denoising problem and apply Theorem 1.

We first remark that since  $A$  is assumed invertible,  $x^0 = A^{-1}y$  and more generally the solution  $x^\alpha$  to (25b) satisfies  $Ax^\alpha = z^\alpha$ , where

$$z^\alpha = \arg \min_{z \in \mathbb{R}^n} \left\{ \frac{1}{2} \|z - y\|^2 + \alpha \mathcal{R}(A^{-1}z) \right\}. \quad (28)$$

By the invertibility of  $A$  and assumptions on  $\mathcal{R}$  it follows that  $\tilde{\mathcal{R}} := \mathcal{R} \circ A^{-1}$  is also convex, bounded below, and continuously differentiable. Furthermore, if we define  $z^* := Ax^*$  notice that

$$\begin{aligned} D_{\mathcal{R}}(x^*, x^0) &= \mathcal{R}(x^*) - \langle \nabla \mathcal{R}(x^0), x^* - x^0 \rangle \\ &= \mathcal{R}(x^*) - \langle A^{-T} \nabla \mathcal{R}(x^0), Ax^* - Ax^0 \rangle \\ &= \tilde{\mathcal{R}}(z^*) - \langle \nabla \tilde{\mathcal{R}}(y), z^* - y \rangle \\ &= D_{\tilde{\mathcal{R}}}(z^*, y). \end{aligned}$$

Thus, assumption (26) reads

$$\mathbb{E} \left[ \tilde{\mathcal{R}}(z^*) - D_{\tilde{\mathcal{R}}}(z^*, y) \right] < \mathbb{E} \left[ \tilde{\mathcal{R}}(y) \right] \quad (29)$$

and assumption (27) reads

$$\mathbb{E} \left[ \tilde{\mathcal{R}}(z^*) \right] < \infty. \quad (30)$$

Using the new notation, the upper level problem (25a) reads

$$\min_{\alpha \in \mathcal{P}} \mathbb{E} \left[ \frac{1}{2} \|z^\alpha - z^*\|^2 \right]. \quad (31)$$

In particular, we have phrased the bilevel learning problem (25) as a denoising bilevel problem (31) and (28) with regularizer  $\tilde{\mathcal{R}}$ . By the properties of  $\tilde{\mathcal{R}}$  and inequalities (29) and (30), it follows from Theorem 1 that 0 is not a solution to (25).  $\square$

## 5 Numerical Experiments

We now explore the presented theory with some numerical examples. Although in practice the problem is high-dimensional, for a geometric and visual interpretation of the theory, we consider in Section 5.1 the small dimensional case of  $n = 2$ . Relevant high-dimensional problems are provided in Section 5.2.

In the following, solutions to the lower level problem are computed either via an analytic closed form solution (where no numerical solver is necessary) or numerically using BFGS [56] for 10000 iterations with backtracking linesearch and early stopping if either the gradient norm evaluates to less than  $10^{-8}$  or a step length smaller than  $10^{-14}$  is considered by backtracking linesearch. We find that early stopping is always achieved. We utilize both the SciPy [72] and ODL [1] Python libraries in our experiments, and our code is available at <https://github.com/s-j-scott/Optimal-Reg-Params-Bilevel>.

### 5.1 Low-dimensional problems

We explore how well the results of Theorem 1 and Theorem 2 characterize positivity in the pointwise setting, that is, we consider Corollary 1 and Corollary 3 respectively. In the following, we consider the area  $\Omega := [-1.6, 1.6] \times [-1.6, 1.6] \subset \mathbb{R}^2$ , discretised into a  $150 \times 150$  grid. Since our results involve  $x^0$  and  $x^*$ , we interpret  $\Omega$  as the reconstruction space, rather than the measurement space.

We fix the ground truth  $x^* = [1, 0.5]^T$ , which will be indicated by a yellow star in the upcoming plots. Considering each point in the grid  $\Omega$  as a candidate  $x^0$ , we compute the boundary for when the relevant inequality of Corollary 1 or Corollary 3 becomes satisfied. If we are in the case  $A = I$ ,

Table 1: Key for the boundary colours used in numerical examples. The shorthand labels used in the following legends are also indicated. Since the results of Corollary 1 and Corollary 3 refer to different bilevel problems, (3) and (10) respectively, we can re-use the label and colour for both boundaries.

Condition satisfied outside the boundary	Colour	Label	Reference
$\mathcal{R}(x^*) < \mathcal{R}(y)$	Red	Old	[27, 28]
$\mathcal{R}(Bx^*) - D_{\mathcal{R}}(Bx^*, x^0) < \mathcal{R}(Bx^0) - D_{\mathcal{R}}(Bx^0, x^0)$	Blue	New	Corollary 1
$\mathcal{R}(x^*) - D_{\mathcal{R}}(x^*, x^0) < \mathcal{R}(x^0)$	Blue	New	Corollary 3
Numerical solution to the bilevel problem is not 0	Black	Numerical	–

we may also compute the boundary for when (5) becomes satisfied. Since the lower level problem requires a measurement  $y$ , in order to have a well defined mapping between the  $x^0$  and  $y$ , we restrict ourselves to invertible  $A$  in this section. We approximate the solution to the bilevel learning problem with data  $(x^*, Ax^0)$  by considering parameters

$$[\alpha_1 = 0, \alpha_2 = 10^{-8}, \dots, \alpha_{99} = 10^3, \alpha_{100} = 10^7],$$

where  $[\log_{10}(\alpha_2), \dots, \log_{10}(\alpha_{99})]$  is a linear discretisation of 98 points between -8 and 3, and select the parameter that achieves the smallest upper level cost. With this, we compute the boundary in  $\Omega$  between the regions where the numerical bilevel solution is zero and strictly positive. A summary of the boundaries and their represented colours and legend names is provided in Table 1.

We consider two forward operators, namely,

$$A_1 = \begin{bmatrix} 1 & 0 \\ 0 & 1 \end{bmatrix} \quad \text{and} \quad A_2 = \begin{bmatrix} 0.7274 & 0.2726 \\ 0.2726 & 0.7274 \end{bmatrix}.$$

For each forward operator, we consider four different regularizers and see how the boundaries, detailed in the above and summarized in Table 1, change. In particular, we consider a general form of Tikhonov and the Huber norm,

$$\mathcal{R}(x) = \frac{1}{2} \|Lx\|^2 \quad \text{and} \quad \mathcal{R}(x) = \sum_{i=1}^p \text{hub}_{\gamma}([Lx]_i)$$

respectively, where  $L \in \mathbb{R}^{p \times n}$ , not necessarily full rank, and

$$\text{hub}_{\gamma}(t) = \begin{cases} |t| - \frac{\gamma}{2} & \text{if } |t| \geq \gamma \\ \frac{1}{2\gamma} t^2 & \text{if } |t| < \gamma. \end{cases}$$

Regarding the choice of  $L$ , we will consider both  $L = I \in \mathbb{R}^{2 \times 2}$ , which will yield standard Tikhonov and Huber norm respectively, and also  $L = [1 \ -1] \in \mathbb{R}^{1 \times 2}$  which can be interpreted as the discretisation of the first-order finite difference operator for  $n = 2$  [44]. For this latter choice of  $L$ , we refer to the regularizers as an  $n = 2$  analogue of the  $H^1$  seminorm and Huber TV respectively.

### 5.1.1 On the characterization of positivity

We are interested in how well Corollary 1 characterizes positivity of solutions of the bilevel learning problem (3). Using the approach outlined above, we can determine the area of the region where the numerical solution to (3) is 0, and also the area where the condition of Corollary 1 is violated.

Should Corollary 1 perfectly characterize positivity, we would expect both areas to coincide. We compute the ratio between these areas for the different  $A$  and  $\mathcal{R}$  mentioned above, and display the results in Table 2. In the denoising setting, we also compute the area where (5) is violated, to see how the new condition compares. In Figure 4a we see that, for Tikhonov denoising, Corollary 1 perfectly characterizes positivity, as we would expect following Example 3. From Table 2, Corollary 1 characterizes the positivity of (3) well for the considered problems, with many area ratios being around 1. Furthermore, we see in Figure 4 and Figure 5 that some instances where the ratio is close to but not exactly 1 is down to numerical error. For the denoising setting, we see in Figure 4 that (5) overestimates the region where 0 is a solution to (3) by a factor of 2 to 4. Compared to condition (5), Corollary 1 yields a better characterization of positivity, particularly for points far away from  $x^*$  - as demonstrated in Figure 4a and Figure 4c.

Table 2: Ratio between the area where 0 is the optimal parameter and area in the reconstruction space where the (old or new) theory condition is violated. Values close to 1 mean the condition is close to fully characterizing positivity of (3). Since (5) is only valid for  $A = I$ , we cannot compare for the  $A \neq I$  case. As we only consider points in  $\Omega$ , if the area where a condition is violated extends beyond  $\Omega$ , we indicate the case with an asterisk beside the provided number. All numbers are given to 3 decimal points.

Problem	Condition violated	Regularizer			
		Tikhonov	$H^1$ seminorm	Huber	Huber TV
Denoising	New	1	1.016*	1.172	0.985*
Denoising	Old	4.008	2.047*	4.207	1.985*
Non-denoising	New	1.028	0.981*	1.181	0.983*
Non-denoising	Old	—	—	—	—

### 5.1.2 Guaranteed positivity for denoising

We now demonstrate the result of Corollary 2, where we are guaranteed that 0 is not a solution provided that  $A = I$ ,  $\mathcal{R}$  is strictly convex, and the noise is additive and of zero mean. We fix ground truth  $x^* = [1, 0]^T$  and generate 1000 noisy realisations by perturbing  $x^*$  with Gaussian noise of mean  $[0, 0]^T$ , standard deviation  $[0.1, 0.1]^T$ . A plot of the ground truth and noisy realisations is shown in Figure 6a. To ensure the regularizer is strictly convex and differentiable, we consider

$$\mathcal{R}(x) = \frac{\beta}{2} \|x\|^2 + \sum_{i=1}^n \text{hub}_{\gamma}(x_i),$$

for  $\beta = \gamma = 0.01$ . For regularization parameters in the linear discretisation of the interval  $[0, 0.1]$  into 50 points, we plot the associated upper level cost in Figure 6b. We see that the optimal parameter is achieved at a strictly positive value. We now show that if the assumption on the noise is violated, we are not guaranteed positivity. For the same  $x^*$  we generate 1000 noisy realisations by perturbing  $x^*$  with Gaussian noise of mean  $[-0.1, 0]^T$  and standard deviation  $[0.1, 0.1]^T$ . A plot of the ground truth and noisy realisations is shown in Figure 6c, and the associated upper level cost in Figure 6d. We see that 0 is the optimal parameter in this case which indicates that the assumption of zero mean noise in Corollary 2 is tight.

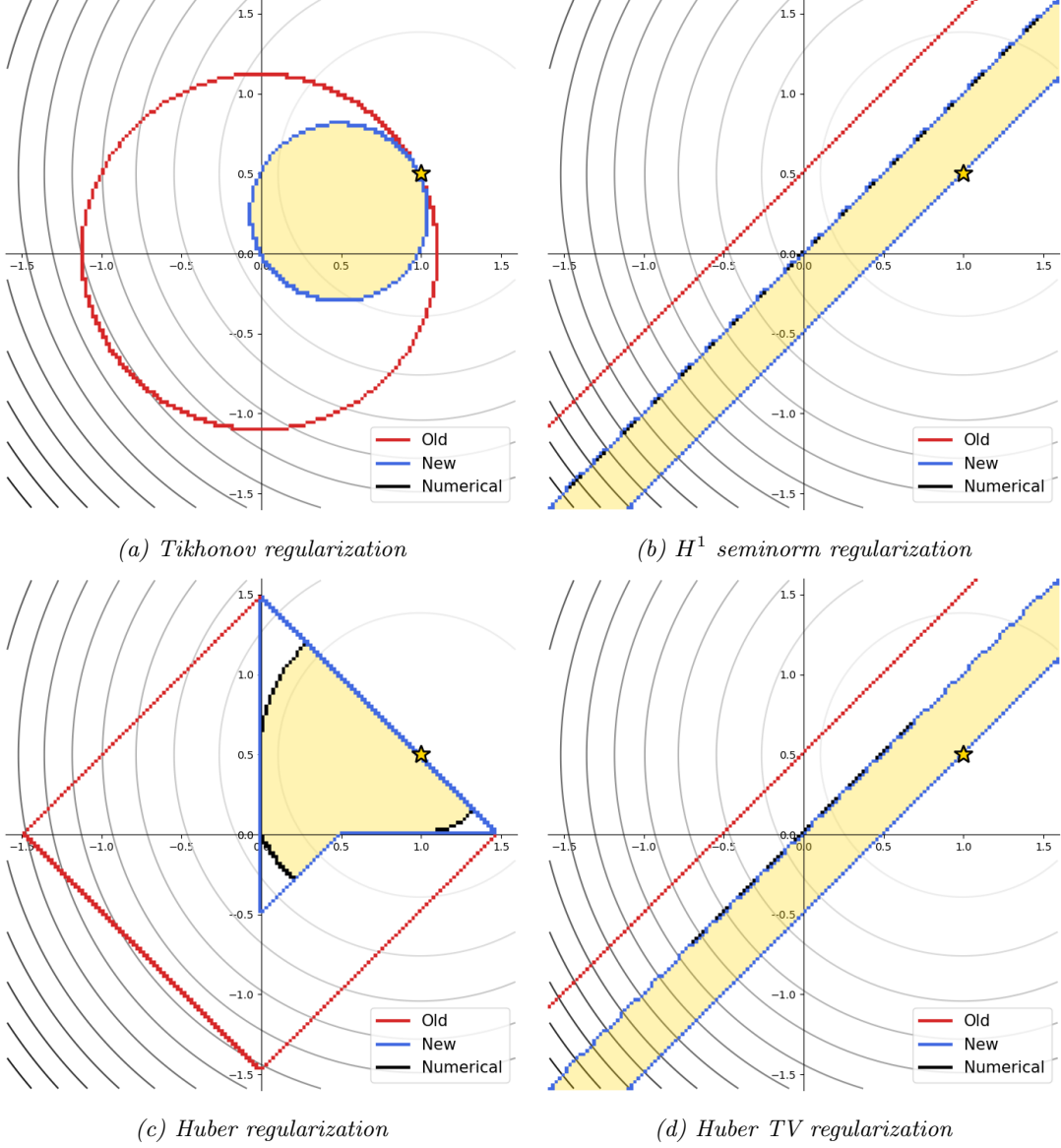


Figure 4: Visualisation of Corollary 1. Plots of the reconstruction space  $\Omega$  for the trivial forward operator ( $A_1$ ) setting and various choices of regularizer, with the condition boundaries as detailed in Table 1. The ground truth  $x^* = [1, 0.5]$  is represented by a yellow star, and level sets of the upper level cost function are visible. The region where 0 is a solution to (3) is shaded yellow. The choice of regularizer is indicated in each subcaption.

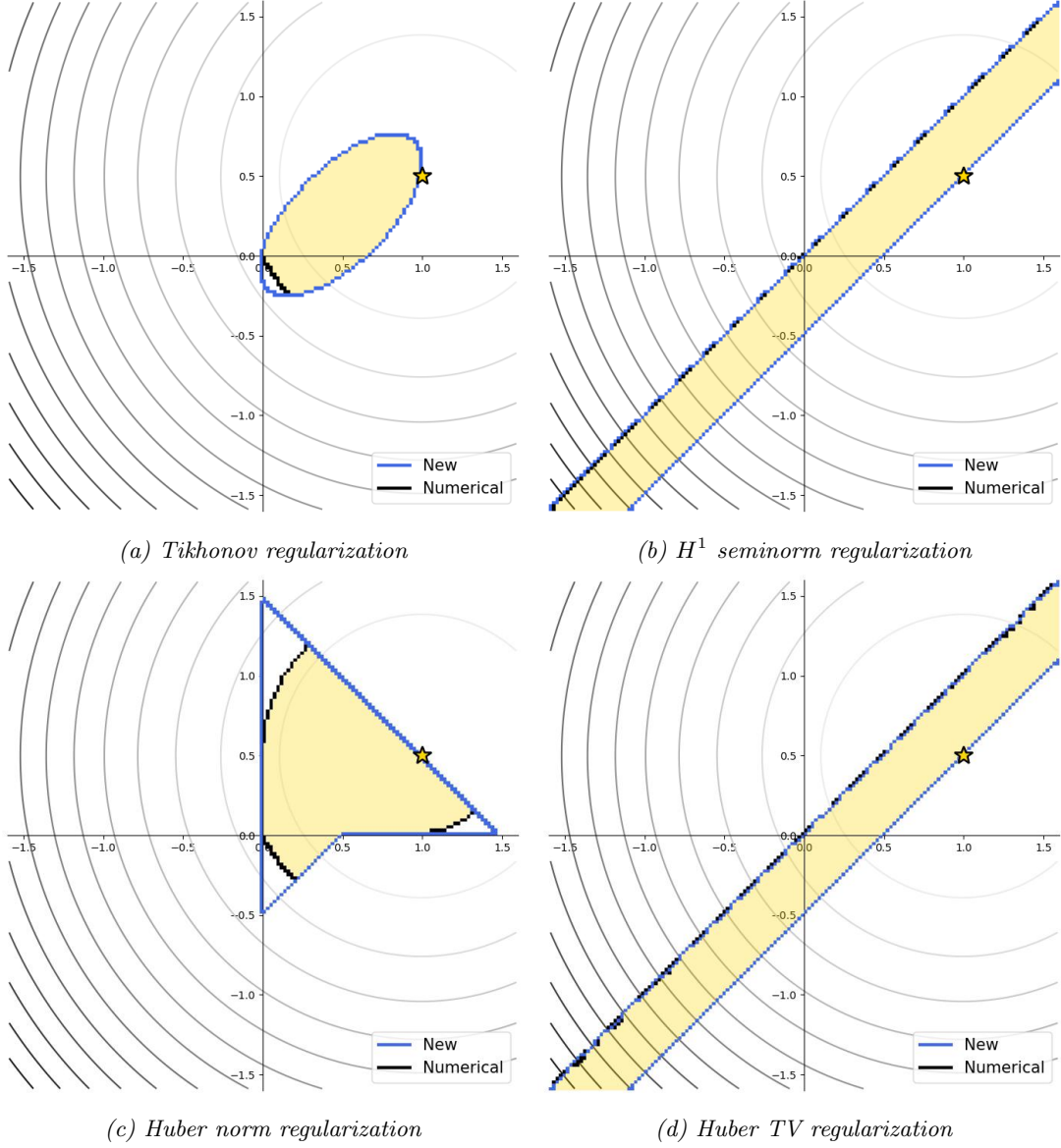


Figure 5: Visualisation of Corollary 1. Plots of the reconstruction space  $\Omega$  for the non-trivial forward operator ( $A_2$ ) setting and various choices of regularizer, with the condition boundaries as detailed in Table 1. The ground truth  $x^* = [1, 0.5]^T$  is represented by a yellow star, and level sets of the upper level cost function are visible. The region where 0 is a solution to (3) is shaded yellow. The choice of regularizer is indicated in each subcaption.

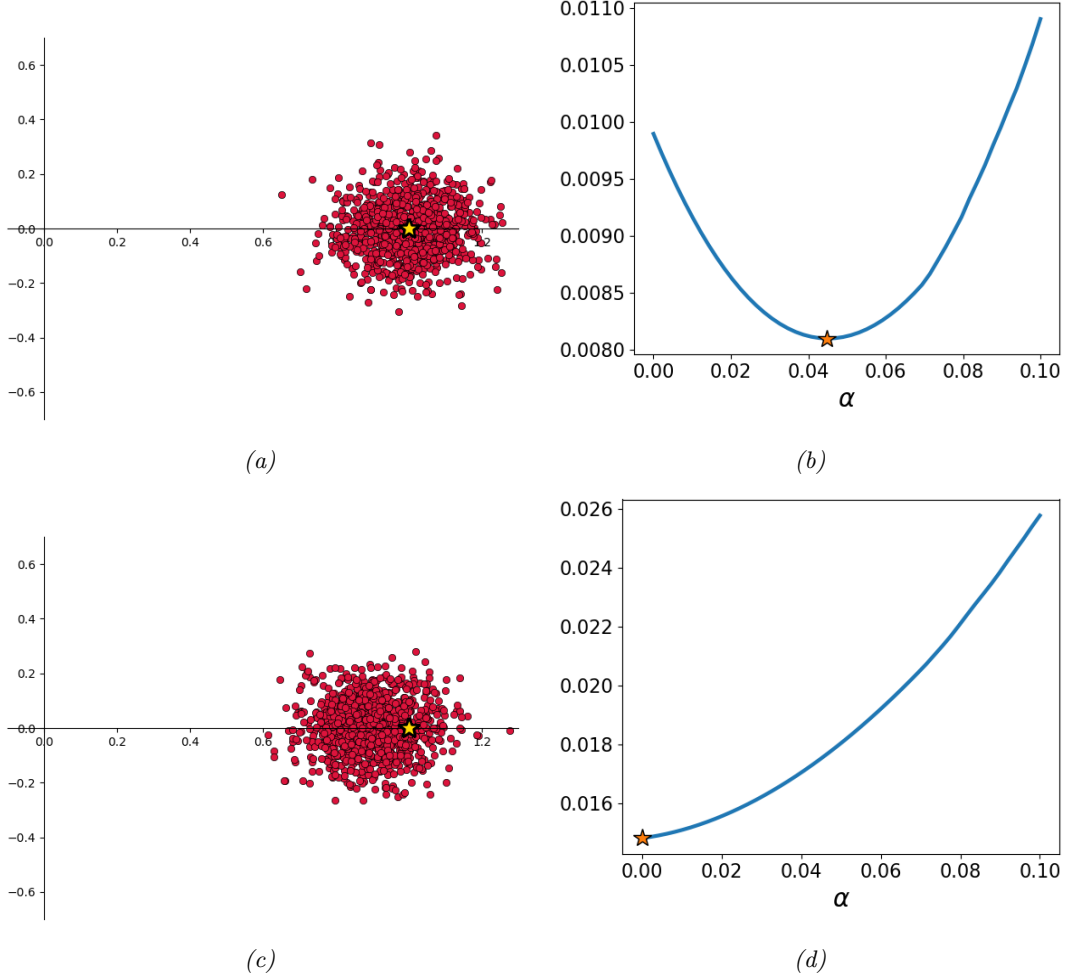


Figure 6: Visualisation of Corollary 2. (a) shows the ground truth  $x^* = [1, 0]^T$  indicated by a yellow star, and 1000 noisy realisations indicated by red dots where the corruption was additive Gaussian noise of mean  $[-0.1, 0]^T$  standard deviation  $[0.1, 0.1]^T$ . (b) shows the squared error upper level cost corresponding to the data in (a). The optimal regularization parameter is indicated by an orange star which, since the conditions of Corollary 2 are satisfied, is guaranteed to not be 0. (c) shows a similar to plot to (a), but the noise has non-zero mean  $[-0.1, 0]^T$ , and so the result of Corollary 2 is not applicable. (d) shows the squared error upper level cost corresponding to the data in (c). The optimal regularization parameter is indicated by an orange star. Since the conditions of Corollary 2 are not satisfied we are not guaranteed that 0 is not a solution to (3). Indeed, 0 is the optimal parameter in this case, indicating that the assumption of zero mean noise in Corollary 2 is tight.

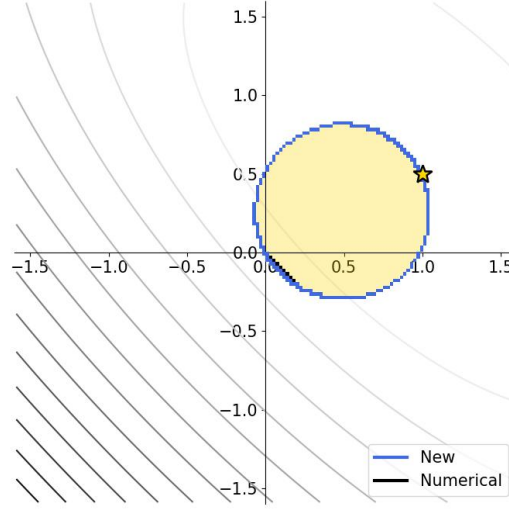


Figure 7: Visualisation of Corollary 3. Plots of the reconstruction space  $\Omega$  for the non-trivial forward operator ( $A_2$ ) setting, Tikhonov regularization, and predictive risk upper level cost. The ground truth  $x^* = [1, 0.5]^T$  is represented by a yellow star, and level sets of the upper level cost function are visible. The region where 0 is a solution to (3) is shaded yellow.

### 5.1.3 Predictive risk upper level

We now demonstrate the result of Corollary 3 where the upper level cost is the predictive risk (10a) without the expectation and  $A$  is invertible. In particular, we consider the same setup as above with forward operator  $A_2$  and Tikhonov regularization. We plot the region for which 0 is a solution and boundary for when the condition of Corollary 3 holds in Figure 7. Since the upper level cost is different to the one considered in the previous numerics, the contour plot of the upper level cost looks very different. We see that the condition of Corollary 3 characterizes whether 0 is a solution to (10) well in this setting. Despite not being the denoising setting, the region for which the condition of Corollary 3 is satisfied is similar in shape to the analogous region in Figure 4a for which the condition of Corollary 1 is satisfied for the case  $A = I$ . This is likely because, due to the invertibility of  $A_2$ , the predictive risk bilevel learning problem (10) is related to a certain denoising bilevel learning problem with the squared error upper level cost.

## 5.2 High-dimensional problems

In this subsection we consider two settings: a denoising scenario where we show that the old condition (5) can fail to capture 0 not being a solution to (3); and a deconvolution scenario where the existing theory is no longer applicable but we can instead employ both Theorem 1 and Theorem 2 in the pointwise setting, that is, Corollary 1 and Corollary 3 respectively.

### 5.2.1 Denoising application

We consider the pointwise denoising setting and provide two examples: one where both the new and old conditions are satisfied, and one where only the new condition is satisfied. We consider the




 (a) Ground truth  $x^*$ 

 (b) Noisy measurement  $y$ 

Figure 8: Relevant data for the large-scale denoising problem. The pixel values are clipped to  $[0, 255]$  where 0 is black and 255 is white. The test image was provided by one of the authors.

$128 \times 128$  pixel ground truth image displayed in Figure 8a and its additive Gaussian noise corrupted version, displayed in Figure 8b, where the noise level,

$$\eta := \frac{\|Ax^* - y\|}{\|Ax^*\|},$$

is chosen to be  $\eta = 0.05$ .

We consider both Huber norm and Huber TV regularization, given by

$$\mathcal{R}(x) = \sum_{i=1}^n \text{hub}_\gamma(x_i) \quad \text{and} \quad \mathcal{R}(x) = \sum_{i=1}^p \text{hub}_\gamma([\nabla x]_i)$$

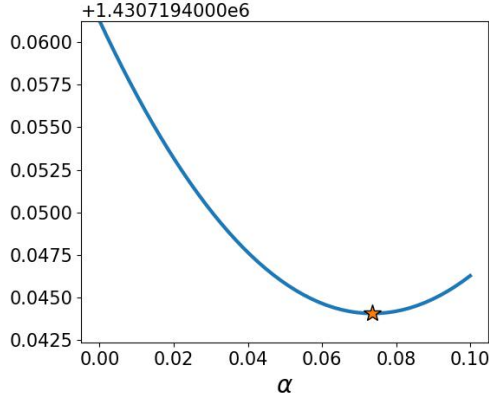
respectively, where  $\nabla$  calculates both the horizontal and vertical gradient of  $x$  and returns the vectorised concatenation of both results. We use the smoothing parameter  $\gamma = 0.01$  in both cases. For Huber norm and Huber TV regularization, we consider parameter spaces  $[0, 0.1]$  and  $[0, 5]$  respectively, linearly discretised into 50 points.

For the Huber norm, we get that  $\mathcal{R}(x^*) = 8051925$  to 7 significant figures (7 s.f.) and  $\mathcal{R}(y) = 8051561$  (7 s.f.) and so the old condition (5) is not satisfied. However, in Figure 9c we see that the optimal regularization parameter is non-zero, despite the associated reconstruction, displayed in Figure 9a, looking similar to the noisy measurement. We remark that the differences in the upper level cost for the considered parameters are very small. The relevant inequality of Corollary 1 is satisfied, reading  $8051514 < 8051560$  (7 s.f.). Thus Corollary 1 successfully captures the fact that 0 is not a solution to the bilevel learning problem, whereas the existing theory is inconclusive.

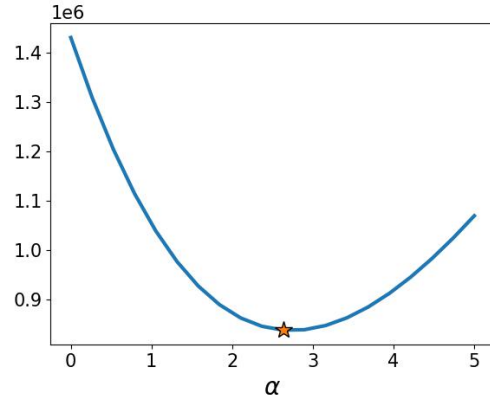
For Huber TV, the assumptions of Corollary 1 and the old condition (5) are both satisfied. In Figure 9d we see that the optimal regularization parameter is non-zero, and the associated reconstruction, displayed in Figure 9b, is an improvement upon on the noisy measurement.



(a) Huber norm reconstruction using the solution to (3),  $\alpha = 0.073$ . (b) Huber TV reconstruction using the solution to (3),  $\alpha = 2.755$ .



(c) Upper level cost for Huber norm regularization

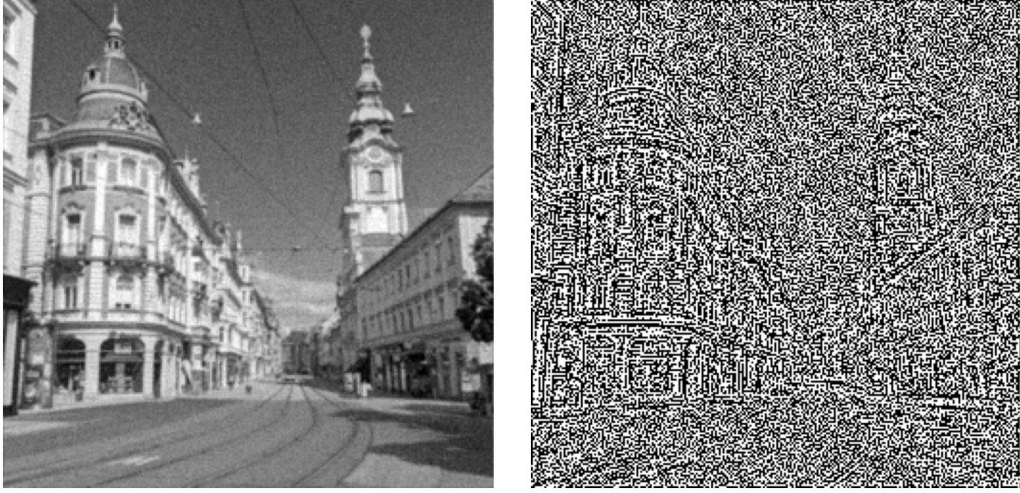


(d) Upper level cost for Huber TV regularization

Figure 9: Visualisation of Corollary 1. Reconstructions and plots of the upper level cost function for the large scale denoising numerical experiment. The pixel values are clipped to  $[0, 255]$  where 0 is black and 255 is white. For Huber norm regularization, despite the old condition being violated, the optimal parameter is non-zero.

### 5.2.2 Deconvolution application

We now consider a pointwise deconvolution problem where the forward operator is a Gaussian blur with standard deviation 1.3. The ground truth image is the same as that of Section 5.2.1 and is displayed in Figure 8a. The observed measurement consists of the blurred ground truth corrupted by additive Gaussian noise of noiselevel  $\eta = 0.05$  and is displayed in Figure 10a. The unregularized reconstruction  $x^0$  is displayed in Figure 10b and is clearly dominated by noise. We consider the


 (a) Corrupted blurry measurement  $y$ 

 (b) Unregularized reconstruction  $x^0$ 

Figure 10: Relevant data for the large-scale deconvolution problem. The pixel values are clipped to  $[0, 255]$  where 0 is black and 255 is white. We see that the unregularized reconstruction is completely dominated by noise.

squared error bilevel problem (3) and also the predictive risk bilevel problem (10) in order to apply both Corollary 1 and Corollary 3. We consider Huber TV regularization, and approximate the solution to (3) by considering the interval  $[0, 3]$  linearly discretised into 50 points and select the parameter that achieves the smallest upper level cost.

We find that the inequalities of Corollary 1 and Corollary 3 are satisfied, with the larger side of the inequality being at least 150 orders of magnitude larger in both cases. This indicates that if the problem is ill-posed and the unregularized reconstruction  $x^0$  is dominated by noise, then the relevant inequalities may be trivially satisfied in practice.

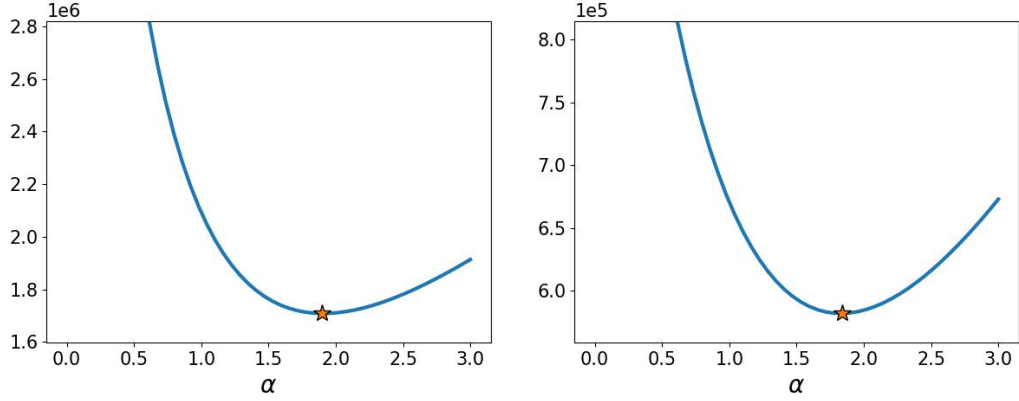
Since both Corollary 1 and Corollary 3 are satisfied we are guaranteed that 0 is not a solution to both the squared error and predictive risk bilevel learning problems, (3) and (10) respectively. Indeed, plots of the corresponding upper level cost functions are displayed in Figure 11c and Figure 11d where we see that both solutions are non-zero. In this instance, both cost functions yield a similar optimal parameter, with the associated reconstructions displayed in Figure 11a and Figure 11b respectively.

## 6 Conclusion

In this work we contributed to the fundamental understanding of bilevel learning as a mathematically sound regularization parameter choice strategy. More precisely, we determined an upper bound of the upper right Dini derivative of the upper level cost function at 0 in terms of Bregman distances and evaluations of the regularizer. In demanding that this upper bound is strictly negative, we established a new sufficient condition to guarantee positivity of solutions of the bilevel learning problem, applicable to settings with an injective forward operator. In addition to this, an extension to the predictive risk cost function was made for an invertible forward operator. Furthermore, we



(a) Huber TV reconstruction using the solution to (3),  $\alpha = 1.895$  (b) Huber TV reconstruction using the solution to (10),  $\alpha = 1.898$



(c) Squared error upper level cost (3a) for Huber TV regularization (d) Predictive risk upper level cost (10a) for Huber TV regularization

Figure 11: Visualisation of Corollary 1 and Corollary 3. Reconstructions, and plots of the upper level cost function for the large scale deblurring numerical experiment. The pixel values are clipped to  $[0, 255]$  where 0 is black and 255 is white. In (c) and (d) we only display upper level cost evaluations that are finite and less than  $10^{300}$ . Since we are not in the denoising setting, the old condition is not applicable but the presented theory successfully identifies that 0 is not a solution to the bilevel problem with both the squared error and predictive risk upper level cost.

showed that in most common denoising problems our condition will always be satisfied and we are guaranteed that 0 is not an optimal regularization parameter. We have shown both analytically and empirically that the presented results characterize positivity well, and are an improvement on a condition commonly used in existing theory.

## Acknowledgements

MJE acknowledges support from EPSRC (EP/S026045/1, EP/T026693/1, EP/V026259/1) and the Leverhulme Trust (ECF-2019-478). The work of SG was partially supported by EPSRC under grant EP/T001593/1. SJS is supported by a scholarship from the EPSRC Centre for Doctoral Training in Statistical Applied Mathematics at Bath (SAMBa), under the project EP/S022945/1.

## References

- [1] J. Adler, H. Kohr, and O. Oktem. Operator discretization library (ODL). Software available from <https://github.com/odlgroup/odl>, vol. 5, 2017.
- [2] Babak Maboudi Afkham, Julianne Chung, and Matthias Chung. Learning Regularization Parameters of Inverse Problems via Deep Neural Networks. *Inverse Problems*, 37(10):105017, 2021.
- [3] Brandon Amos, Lei Xu, and J. Zico Kolter. Input Convex Neural Networks. In *Proceedings of the 34th International Conference on Machine Learning*, volume 70 of *ICML '17*, page 146–155. JMLR, 2017.
- [4] Qamrul Hasan Ansari, Lalitha C. S., and Monika Mehta. General Convexity, Nonsmooth Variational Inequalities, and Nonsmooth Optimization. *CRC Press, Boca Raton, 1st edn.*, 2014.
- [5] Stephan W. Anzengruber and Ronny Ramlau. Morozov’s discrepancy principle for Tikhonov-type functionals with nonlinear operators. *Inverse Problems*, 26(2):025001, 2010.
- [6] Simon Arridge, Peter Maass, Ozan Öktem, and Carola-Bibiane Schönlieb. Solving inverse problems using data-driven models. *Acta numerica*, 28:1–174, 2019.
- [7] Anatolii B. Bakushinskii. Remarks on choosing a regularization parameter using the quasi-optimality and ratio criterion. *USSR Computational Mathematics and Mathematical Physics*, 24(4):181–182, 1984.
- [8] Amir Beck. First-Order Methods in Optimization. *MOS-SIAM Series on Optimization. Society for Industrial and Applied Mathematics, Philadelphia, Pennsylvania*, 2017.
- [9] Martin Benning and Martin Burger. Modern regularization methods for inverse problems. *Acta numerica*, 27:1–111, 2019.
- [10] Martin Benning, Marta M. Betcke, Matthias J. Ehrhardt, and Carola-Bibiane Schönlieb. Gradient descent in a generalised Bregman distance framework. *Geometric Numerical Integration and Its Applications, MI Lecture Notes* 74:40–45, 2017.
- [11] Thomas Bonesky. Morozov’s discrepancy principle and Tikhonov-type functionals. *Inverse Problems*, 25(1):015015, 2009.
- [12] Kristian Bredies, Martin Holler. Higher-order total variation approaches and generalisations. *Inverse Problems*, 36(12):123001, DOI: 10.1088/1361-6420/ab8f80, 2020.
- [13] Kristian Bredies, Karl Kunisch, Thomas Pock. Total Generalized Variation. *SIAM Journal on Imaging Sciences*, 3(3):492–526, 2010.

- [14] Martin Burger. Bregman Distances in Inverse Problems and Partial Differential Equations In *Hiriart-Urruty, JB., Korytowski, A., Maurer, H., Szymkat, M. (eds) Advances in Mathematical Modeling, Optimization and Optimal Control*. Springer Optimization and Its Applications, vol 109. Springer, Cham. DOI: 10.1007/978-3-319-30785-5\_2, 2016.
- [15] Martin Burger, Elena Resmerita, and Lin He. Error estimation for Bregman iterations and inverse scale space methods in image restoration. *Computing*, 81(2/3):109–136, November 2007.
- [16] James Bergstra and Yoshua Bengio. Random search for hyper-parameter optimization. *Journal of Machine Learning Research*, 13:281–305, 2012.
- [17] Yair Censor and A. Lent. An iterative row-action method for interval convex programming. *Journal of Optimization Theory and Applications*, 34:321–353, 1981.
- [18] Antonin Chambolle and Pierre-Louis Lions. Image recovery via total variation minimization and related problems. *Numer. Math.* 76, 167–188, DOI: 10.1007/s002110050258, 1997.
- [19] Antonin Chambolle and Thomas Pock. An introduction to continuous optimization for imaging. *Acta numerica*, 25:161–319, 2016.
- [20] Yunjin Chen, Thomas Pock, René Ranftl, and Horst Bischof. Revisiting Loss-Specific Training of Filter-Based MRFs for Image Restoration. *Lecture notes in computer science*, 8142:271–281, 2014.
- [21] Julianne Chung, Sarah Knepper, and James G. Nagy. Large-Scale Inverse Problems in Imaging. In *Handbook of Mathematical Methods in Imaging*, pages 43–86. Springer New York, New York, NY, 2011.
- [22] Julianne Chung, Matthias Chung, Silvia Gazzola, Mirjeta Pasha. Efficient learning methods for large-scale optimal inversion design. In *Numerical Algebra, Control and Optimization*, DOI: 10.3934/naco.2022036, 2022
- [23] Benoît Colson, Patrice Marcotte, and Gilles Savard. An overview of bilevel optimization. *Annals of Operations Research*, 153(1):235–256, 2007.
- [24] Caroline Crockett and Jeffrey A. Fessler. Bilevel Methods for Image Reconstruction, volume 15 of *Foundations and Trends® in Signal Processing*, 2022.
- [25] Bernard Dacorogna. Direct Methods in the Calculus of Variations, volume 78 of *Applied Mathematical Sciences*. Springer New York, New York, NY, 2nd edn., 2008.
- [26] Gianni Dal Maso. An Introduction to  $\Gamma$ -convergence. *Progress in Nonlinear Differential Equations and their Applications*. vol 8. Birkhäuser, Boston, MA. 1993
- [27] Elisa Davoli, Rita Ferreira, Carolin Kreisbeck, and Hidde Schönberger. Structural changes in nonlocal denoising models arising through bi-level parameter learning. *Applied mathematics & optimization*, 88(1):9, 2023.
- [28] Juan Carlos De los Reyes, Carola-Bibiane Schönlieb, and Tuomo Valkonen. The structure of optimal parameters for image restoration problems. *Journal of mathematical analysis and applications*, 434(1):464–500, 2016.

- [29] Juan Carlos De los Reyes, Carola-Bibiane Schönlieb, and Tuomo Valkonen. Bilevel parameter learning for higher-order total variation regularisation models. *Journal of mathematical imaging and vision*, 57(1):1–25, 2017.
- [30] Charles-Alban Deledalle, Samuel Vaiter, Jalal Fadili, and Gabriel Peyré. Stein Unbiased GrAdient estimator of the Risk (SUGAR) for Multiple Parameter Selection *SIAM Journal on Imaging Sciences* 7(4):2448–2487, DOI: 10.1137/140968045, 2014
- [31] Matthias J. Ehrhardt and Lindon Roberts. Inexact Derivative-Free Optimization for Bilevel Learning. *Journal of mathematical imaging and vision*, 63(5):580–600, 2021.
- [32] Matthias J. Ehrhardt and Lindon Roberts. Analyzing Inexact Hypergradients for Bilevel Learning. *arXiv preprint arXiv:2301.04764*, 2023.
- [33] Heinz Werner Engl, Martin Hanke, and Andreas Neubauer. Regularization of Inverse Problems. *Mathematics and Its Applications. Springer*, 1996.
- [34] Jérôme Fehrenbach, Mila Nikolova, Gabriele Steidl, and Pierre Weiss. Bilevel Image Denoising Using Gaussianity Tests. *Home Scale Space and Variational Methods in Computer Vision SSVM 2015.*, 9087:117–128, DOI: 10.1007/978-3-319-18461-6\_10, 2015
- [35] Silvia Gazzola and Malena Sabaté Landman. Krylov methods for inverse problems: Surveying classical, and introducing new, algorithmic approaches. *GAMM-Mitteilungen*, 43(4), 202000017, 2020
- [36] Silvia Gazzola and Paolo Novati. Automatic parameter setting for Arnoldi–Tikhonov methods. *Journal of Computational and Applied Mathematics* 256:0377–0426, DOI: 10.1016/j.cam.2013.07.023, 2014
- [37] Jonas Geiping and Michael Moeller. Parametric Majorization for Data-Driven Energy Minimization Methods. In *2019 IEEE/CVF International Conference on Computer Vision (ICCV)*. IEEE, 2019.
- [38] Guy Gilboa and Stanley Osher. Nonlocal operators with applications to image processing *Multiscale modeling & simulation* 7(3):1005–1028, Siam Publications, 2008
- [39] Giorgio Giorgi and Sándor Komlós. Dini derivatives in optimization - Part I, volume 15 of *Decisions in Economics and Finance*. Springer, 1992.
- [40] Mark S. Gockenbach and Elaheh Gorgin. On the convergence of a heuristic parameter choice rule for Tikhonov regularization. *SIAM Journal on Scientific Computing*, 40(4):A2694–A2719, 2018.
- [41] Gene H. Golub, Michael Heath, and Grace Wahba. Generalized Cross-Validation as a Method for Choosing a Good Ridge Parameter. *Technometrics*, 21(2):215–223, 1979.
- [42] Jacques S. Hadamard. Sur les problemes aux derive espartielles et leur signification physique. In *Princeton University Bulletin*, pages 49–52, 1902.
- [43] Per Christian Hansen. Discrete inverse problems : insight and algorithms. *Fundamentals of algorithms. Society for Industrial and Applied Mathematics, Philadelphia, Pa.*, 2010.

- [44] Per Christian Hansen, James G. Nagy, and Dianne P. O’Leary. Deblurring images : matrices, spectra, and filtering. *Fundamentals of algorithms. Society for Industrial and Applied Mathematics*, 2006.
- [45] Michael Hintermüller, Kostas Papafitsoros, Carlos N. Rautenberg, and Hongpeng Sun. Dualization and Automatic Distributed Parameter Selection of Total Generalized Variation via Bilevel Optimization. *Numerical Functional Analysis and Optimization*, 43(8):887–932, DOI: 10.1080/01630563.2022.2069812, 2022.
- [46] Gernot Holler, Karl Kunisch, and Richard C. Barnard. A Bilevel Approach for Parameter Learning in Inverse Problems. *Inverse Problems*, 34(11):115012, 2018.
- [47] Peter J. Huber. Robust Estimation of a Location Parameter. *The Annals of Mathematical Statistics*, 35(1):73 – 101, 1964.
- [48] Bangti Jin and Peter Maass. Sparsity regularization for parameter identification problems. *Inverse Problems*, 28(12):123001–70, 2012.
- [49] Bangti Jin, Dirk A. Lorenz, and Stefan Schiffler. Elastic-net regularization: error estimates and active set methods. *Inverse Problems*, 25(11):115022, 2009.
- [50] R. Kannan and Carole King Kreuger. Advanced Analysis on the Real Line. *Universitext. Springer*, 1996.
- [51] Steven G Krantz and Harold R Parks. The Implicit Function Theorem. *Springer, New York*, 2012.
- [52] Karl Kunisch and Thomas Pock. A Bilevel Optimization Approach for Parameter Learning in Variational Models. *SIAM Journal on Imaging Sciences*, 6(2):938–983, 2013.
- [53] Andreas Langer. Automated Parameter Selection for Total Variation Minimization in Image Restoration. *Journal of Mathematical Imaging and Vision*, 57(2):239–268, DOI: 10.1007/s10851-016-0676-2, 2017.
- [54] Andrew Markoe. The Radon Transform. In *Analytic Tomography*, Encyclopedia of Mathematics and its Applications, pages 58-126, Cambridge: Cambridge University Press. DOI: 10.1017/CBO9780511530012.003, 2006.
- [55] Subhadip Mukherjee, Sören Dittmer, Zakhar Shumaylov, Sebastian Lunz, Ozan Öktem, and Carola-Bibiane Schönlieb. Learned convex regularizers for inverse problems. *arXiv preprint arXiv:2008.02839*, 2020.
- [56] Jorge Nocedal and Stephen J. Wright. Numerical Optimization. *Springer New York*, 2nd edn., 2006.
- [57] Johan Nuyts, Dirk Bequé, Patrick Dupont, and L. Mortelmans. A concave prior penalizing relative differences for maximum-a-posteriori reconstruction in emission tomography. *IEEE Transactions on Nuclear Science*, 49(1):56–60, 2002.
- [58] Peter Ochs, René Ranftl, Thomas Brox, and Thomas Pock. Techniques for Gradient-Based Bilevel Optimization with Non-smooth Lower Level Problems. *J Math Imaging Vis* 56:175–194, DOI: 10.1007/s10851-016-0663-7, 2016.



- [59] Peter Ochs, René Ranftl, Thomas Brox, and Thomas Pock. Bilevel optimization with nonsmooth lower level problems. In *International Conference on Scale Space and Variational Methods in Computer Vision (SSVM)*, 2015.
- [60] Konstantinos Papafitsoros and Carola-Bibiane Schönlieb. A Combined First and Second Order Variational Approach for Image Reconstruction, *Journal of Mathematical Imaging and Vision*. 48(2):308-338, DOI: 10.1007/s10851-013-0445-4, 2014.
- [61] Juan Peypouquet. Convex Optimization in Normed Spaces : Theory, Methods and Examples, volume 0 of *SpringerBriefs in Optimization*. Springer, 1st edn., 2015.
- [62] Eric T. Quinto. An introduction to X-ray tomography and Radon transforms. In *The Radon Transform and Applications to Inverse Problems*, volume 63 of *AMS Proceedings of Symposia in Applied Mathematics*, pages 1-23, 2018.
- [63] Sidney I. Resnick. A Probability Path. *Modern Birkhäuser Classics*. Birkhäuser, 1st edn., 2014.
- [64] Wolfgang Ring. Structural Properties of Solutions to Total Variation Regularization Problems. *ESAIM: Mathematical Modelling and Numerical ANalysis* 32(4):799-810 DOI: 10.1051/m2an:2000104, 2000.
- [65] Ralph Tyrell Rockafellar. Convex Analysis. *Princeton Landmarks in Mathematics and Physics*, 1970.
- [66] Leonid I. Rudin, Stanley Osher, and Emad Fatemi. Nonlinear total variation based noise removal algorithms. *Physica D: Nonlinear Phenomena*, 60(1):259-268, 1992.
- [67] Kegan G. G. Samuel and Marshall F. Tappen. Learning Optimized MAP Estimates in Continuously-Valued MRF Models *2009 IEEE Conference on Computer Vision and Pattern Recognition*, pages 477-484, 2009
- [68] Pan Shang and Lingchen Kong. Regularization Parameter Selection for the Low Rank Matrix Recovery. *Journal of Optimization Theory and Applications*, 189(3):772-792, 2021.
- [69] Ferdia Sherry, Martin Benning, Juan Carlos De los Reyes, Martin J. Graves, Georg Maierhofer, Guy Williams, Carola-Bibiane Schönlieb, and Matthias J. Ehrhardt. Learning the sampling pattern for MRI. *IEEE Transactions on Medical Imaging*, 39(12):4310–4321, 2020.
- [70] Ankur Sinha, Pekka Malo, and Kalyanmoy Deb. A Review on Bilevel Optimization: From Classical to Evolutionary Approaches and Applications. *IEEE transactions on evolutionary computation*, 22(2):276–295, 2018.
- [71] Bruno Sixou. Adaptative regularization parameter for Poisson noise with a bilevel approach: application to spectral computerized tomography. *Inverse Problems in Science and Engineering*, 29(11):1519-1536, DOI: 10.1080/17415977.2020.1864348, 2021.
- [72] Pauli Virtanen, Ralf Gommers, Travis E. Oliphant, et al. SciPy 1.0: fundamental algorithms for scientific computing in Python. *Nature Methods*, 17:261-272, DOI: 10.1038/s41592-019-0686-2, 2020.
- [73] Brendt Wohlberg and Paul Rodriguez. An Iteratively Reweighted Norm Algorithm for Minimization of Total Variation Functionals. *IEEE Signal Processing Letters* 14(12):948-951, DOI: 10.1109/LSP.2007.906221, 2007

- [74] Han Zhang, Xuefeng Chen, Xiaoli Zhang, and Xinrong Zhang. A Bi-Level Nested Sparse Optimization for Adaptive Mechanical Fault Feature Detection. *IEEE Access* 8:19767-19782, DOI: 10.1109/ACCESS.2020.2968726, 2020.
- [75] Nicolas Zucchet and João Sacramento. Beyond backpropagation: bilevel optimization through implicit differentiation and equilibrium propagation. *arXiv preprint* arXiv:2205.03076, 2022.